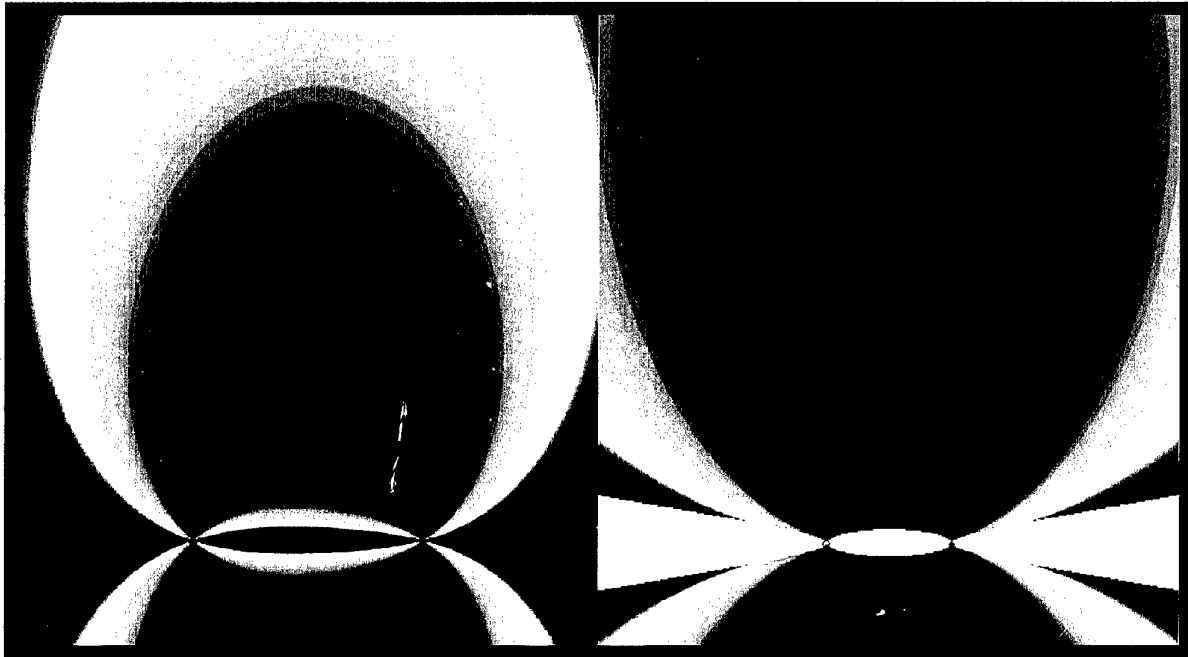


# SACLANT UNDERSEA RESEARCH CENTRE REPORT



**DISTRIBUTION STATEMENT A**  
Approved for Public Release  
Distribution Unlimited

20000609 067

DATA QUALITY INSPECTED

## Target Localization with Multiple Sonar Receivers

L. Mozzone, P. Lorenzelli

The content of this document pertains to work performed under Project 04-B of the SACLANTCEN Programme of Work. The document has been approved for release by The Director, SACLANTCEN.



Jan L. Spoelstra  
Director

**DISTRIBUTION STATEMENT A**  
Approved for Public Release  
Distribution Unlimited

intentionally blank page

**Deployable Underwater Surveillance Systems.  
Target localization with multiple sonar receivers.**

L. Mozzone, P. Lorenzelli

**Executive Summary:**

Deployable Underwater Surveillance Systems (DUSS) are an active sonar concept based on a distributed network of small autonomous nodes (transmitters / receivers) integrated into a multistatic system. One of the challenges of integrating diverse receivers into a single sonar system is the consistent measurement of contact positions. Once the consistency problem is solved (SR-291), improved target localization accuracy is provided by the geometric separation of receivers.

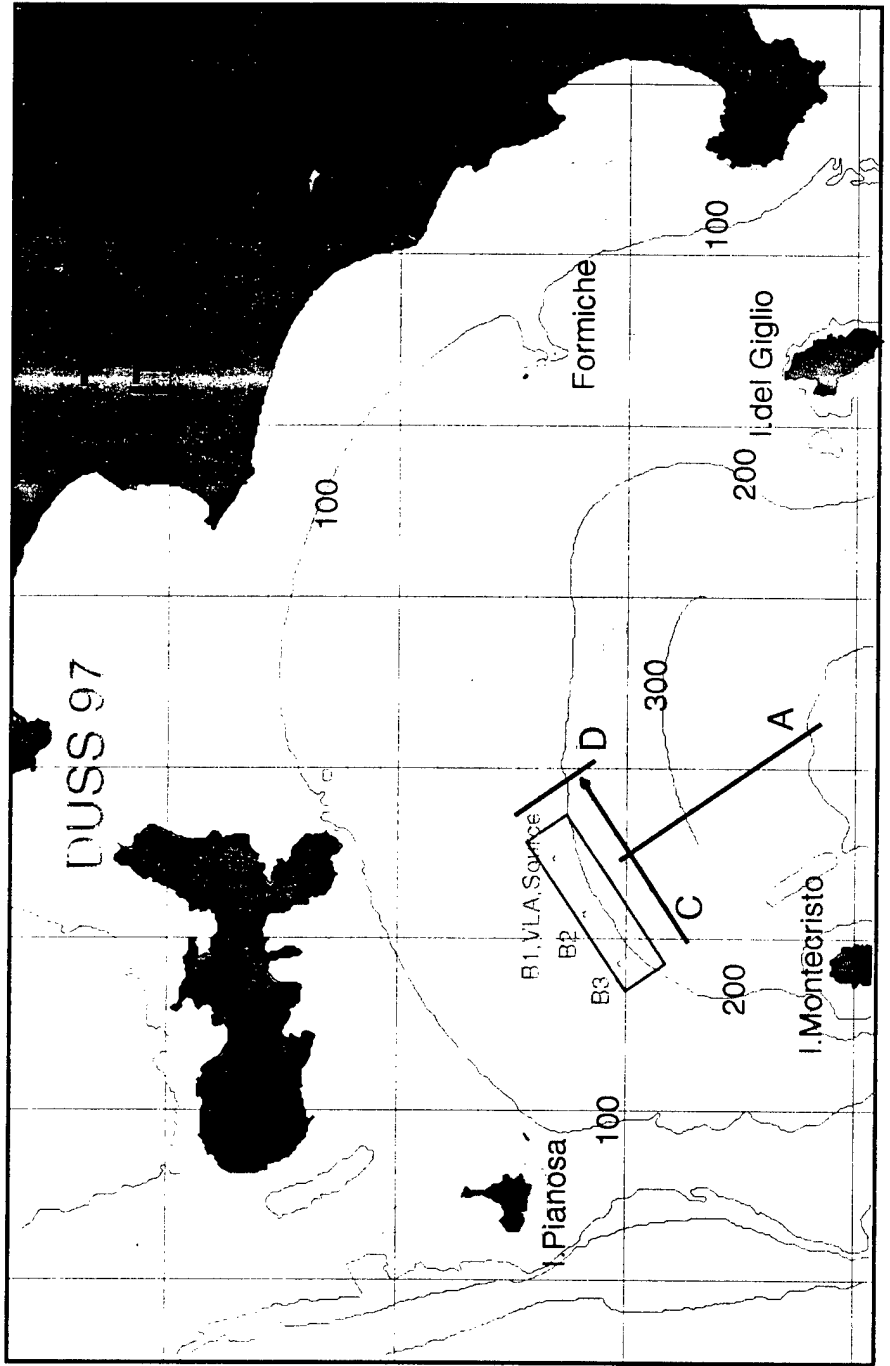
This study initially assesses the target localization performance of individual DUSS sonar nodes based on data collected during the "DUSS'97" trial. Detection performance and system design issues are addressed in previous reports. Because time information is more accurate and cheaper than bearing information, the precision of target localization methods based only on time of echo arrival is investigated ("Tri-lateration"). Monte Carlo simulations estimate the performance of such methods from experimental inputs. Results are validated by comparison with real data. Localization precision spans a wide range of values, according to target position. It is best around the symmetry axis passing between the buoys, also at relatively long ranges. Summary results are referred to discrete points in that area.

- The performance obtained from a pair of buoys with time - of arrival of echoes is considered first. An error better than 150 m at 10 km, 270 m at 20 km is obtained.
- This method achieves important performance improvements versus classical time - and - bearing localization with a single receiver (66 % of the errors) with wide inter - receivers spacing (8 n.mi) With only 4 n.mi spacing, performance is comparable up to ranges of 10 km, 20 % worse at 20 km.
- Three buoys are then considered. The resulting combination yields further error reductions between 8 % and 42 %. Errors are better than 115 m up to 16 km away from the centre of the buoys, and 89 m at the centre.
- The same principle is applied to the localization of an Autonomous Underwater Vehicle (AUV) with a synchronized FM pinger on board. An accuracy better than 83 m is obtained within 10 km of the buoys.
- Because the system can also be operated passively, the case of bearings - only localization with two buoys is addressed. Expected errors are 250 m at 10 km with 4° beams.

Finally, the dependence of localization errors on such system parameters as compass accuracy, buoy separation, buoy localization, and on the accuracy of environmental modelling is addressed for the three different localization methods.

- Existing compass accuracy is satisfactory ( $0.35^\circ$  digitization).
- A buoy separation of 8 n.mi is recommended for all methods. Localization errors decrease by up to 45 % passing from 4 n.mi to 8 n.mi separation.
- A  $\sigma$  of 20 m for buoy localization is acceptable and contributes to 16 - 25 % of measured errors.
- Acoustic modelling is necessary in order to compute the travel time along acoustic propagation paths. If not used, it contributes another 70 % of measured errors. Very accurate modelling is recommended but not crucial (20 % of errors).
- Beams of  $4^\circ$  are recommended for accurate passive operation.

Further to the above indications on system design, the study of tracking and inter - buoy data fusion are also recommended in order to proceed towards a complete assessment of the operational potentials of DUSS.



**Deployable Underwater Surveillance Systems.  
Target localization with multiple sonar receivers.**

L. Mozzone, P. Lorenzelli\*

**Abstract:** Deployable Underwater Surveillance Systems (DUSS) are a network of small multistatic transmitter / receiver sonar nodes. This study analyzes the contact localization capabilities of DUSS in term of range, time and bearing error. This information is used in Monte Carlo simulations to estimate the accuracy of multistatic localization methods using 2 or 3 receivers. Simulations are validated by real data. Time – only localization of active sonar echoes with 2 receivers produces error estimates of 150 m at 10 km. Active pinger localization with 2 receivers produces average errors of 83 m at 10 km. Bearings – only passive localization with 2 receivers produces average errors of 250 m at 10 km. Buoy separation, buoy localization accuracy, acoustic travel time estimation, beam width and compass accuracy are the most critical system parameters. The use of three receivers further improves accuracy.

**Keywords:** Range -Time - Bearing - Localization - Multistatic - Sonar - Modelling - Experiment - AUV.

**Acknowledgments**

The authors wish to thank S. Bongi, the Engineering Technical Division staff, and the Masters, Officers and Crews of *NRV Alliance*, *NRV Manning* and *ITN Ponza* for their vital contribution to this study.

---

\* Università degli Studi Pisa, Facoltà di Ingegneria Informatica

## Contents

1. Introduction .....	1
2. Cramer Rao lower bound of localization errors.....	2
2.1 <i>Signal to noise ratio and direction estimation</i> .....	2
2.2 <i>Signal to noise ratio and time-of-arrival estimation</i> .....	3
3. Data Analysis.....	4
3.1 <i>Experimental data</i> .....	5
3.2 <i>Summary of results</i> .....	8
3.3 <i>Discussion</i> .....	9
3.4 <i>Conclusions</i> .....	10
4. Integrated target localization with multistatic active sonar: 2 receivers, time only .....	12
4.1 <i>Time-only localization with 2 receivers</i> .....	12
4.2 <i>Influence of system parameters on time-only localization</i> .....	15
4.3 <i>Comparison of time-only, 2 receivers versus time-and-bearing, 1 receiver</i> ... 22	
4.4 <i>Comments on time – only localization with 2 receivers..</i> .....	22
5. Integrated target localization with multistatic passive sonar: 2 receivers.....	24
5.1 <i>Tri-angulation localization system</i> .....	24
5.2 <i>Time-only localization of AUV with 2 receivers</i> .....	29
5.3 <i>Conclusions</i> .....	30
6. Target localization with three sensors .....	31
6.1 <i>Time only-localization: tri-lateration</i> .....	31
6.2 <i>AUV time - only localization</i> .....	33
6.3 <i>Conclusions</i> .....	34
7. Conclusions and recommendations .....	35
8. References .....	37
Annex A – Equation of models .....	39
Annex B – Contact localization data .....	46

## Introduction

---

Deployable Underwater Surveillance Systems (DUSS) consist of a distributed network of **multistatic active** sonar transmitters and receivers. They are autonomous, **small**, potentially low cost and/or expendable. The system is optimized for operation in **shallow** and coastal waters against **small targets**, in the presence of heavy shipping **traffic** and strong **reverberation**. The objective of this project is the investigation and assessment of performance potentials of the DUSS concept by means of experimental campaigns conducted with a test system, and the final formulation and trial of an optimized concept demonstrator. The characteristics of the experimental system and the results of tests at sea, quantifying the detection performance of DUSS are summarized in [1,2,3,4].

The present study pursues the following objectives:

- Analyze target localization performance of individual deployable receivers in terms of time and bearing information.
- Evaluate by means of simulations the expected performance of various multistatic localization techniques.
- Identify the parameters characterizing target error localization and quantify their influence on the different localization techniques.
- Provide system design guidance and the basis for further studies on target localization, tracking and inter-receiver contact fusion.

The Multistatic localization techniques described here benefit from the geometric separation between receivers, but require an efficient inter – receiver association of contacts. The feasibility of this concept has been addressed and demonstrated in [4], and requires directivity at the receivers.

Detection performance and system design issues are addressed in previous reports [1-3]. The necessity and extent of receiver directivity required for efficient contact detection and association is not studied here.

The following sections review theoretical bounds of localization accuracy (Section 2), analyze experimental data (Section 3), apply the results to models of three different localization techniques using two receivers (Section 4, 5) or three receivers (Section 6). Conclusions and recommendations for further work are finally drawn (Section 7).

## 2

## Cramer Rao lower Bounds of localization errors

This section addresses target localization errors of DUSS receivers (either monostatic or bistatic) when operated individually. The integrated use of separate receivers and the benefits of their geometrical separation are addressed in Sections 4 – 7. Both bearing and time of arrival of echoes are considered. The effect of limited SNR of echoes is shown by means of the classical Cramer Rao Lower Bounds (CRLB) formulas. As shown by the following tables, most target localization errors are produced by direction estimation variance  $\sigma_\theta$ , followed by  $\sigma_\tau$  (for ranges beyond 1 km).

### 2.1 Signal to Noise Ratio and direction estimation

Signal to noise ratio (SNR) is an important parameter determining bearing estimation accuracy. Noise interacts with the beampattern and introduces a random perturbation in the apparent direction of the maximum of SNR. The Cramer Rao bound formula estimates the lower bound for the standard deviation of direction estimation [6]:

$$\sigma_\theta = \frac{\lambda}{\sqrt{SNR_{out}} \cdot L} \quad (2.1)$$

where  $\lambda$  is the wave length,  $SNR_{out}$  is computed at the sonar output and  $L$  is the RMS array aperture length. For a simple linear array of length  $l$ :  $L = \pi l / \sqrt{3}$ . An array with  $l = 3$  m provides the same -3 dB beamwidth of the receivers used here ( $13^\circ$  at 1.9 kHz and  $7^\circ$  at 3.5 kHz).

**Table 1** Cramer Rao lower bounds for the present experiments.

Freq. (Hz)	SNR (dB)	$\sigma_\theta$ (deg)
1900	6	4.2
	12	2.1
	20	0.8
	25	0.5
3500	6	2.3
	12	1.1
	20	0.5
	25	0.25

**2.2 Signal to Noise Ratio and time-of-arrival estimation**

The classical Cramer Rao formula also computes the lower bound for the standard deviation of time delay estimation [6]:

$$\sigma_{\tau} = \frac{1}{\sqrt{SNR_{out} \cdot \beta}} \tag{2.2}$$

where SNRout is computed at the sonar output and  $\beta$  is RMS bandwidth of the signal (200 Hz in the experiments and in the table below).

**Table 2 Cramer Rao lower bounds for the present experiments.**

SNR (dB)	$\sigma_{\tau}$ (ms)	$\sigma_{\tau}^*$ (m)	$\sigma_{\tau}^{**}$ (m)
6	2.5	1.9	3.8
12	1.25	0.9	1.8
20	0.5	0.4	0.8

\*Monostatic case with c=750 m/sec  
 \*\* Bi-static case with c=1500 m/sec

## 3

## Data Analysis

The present section analyses the data collected by three receivers with an echo repeater target during experimental runs of the DUSS'97 campaign [1, 2, 3, 4]. The use of a digital echo repeater simulating a Target Strength value of 30 dB produces results independent from noise effects. The typical system characteristics of individual DUSS units can therefore be analyzed. Target acoustic localization precision of DUSS receivers is measured in terms of echo bearing and time of arrival estimation. The real target position is obtained with the Differential Global Positioning System (DGPS), which is very precise, with a standard deviation of 5 m [7]. The displacement between GPS antenna on the towing vessel and the towed body of the Echo Repeater is compensated taking into account tow depth, speed, and course. Figure 1 below shows the geometry of the tests and the target trajectory types "A", "C", "D".

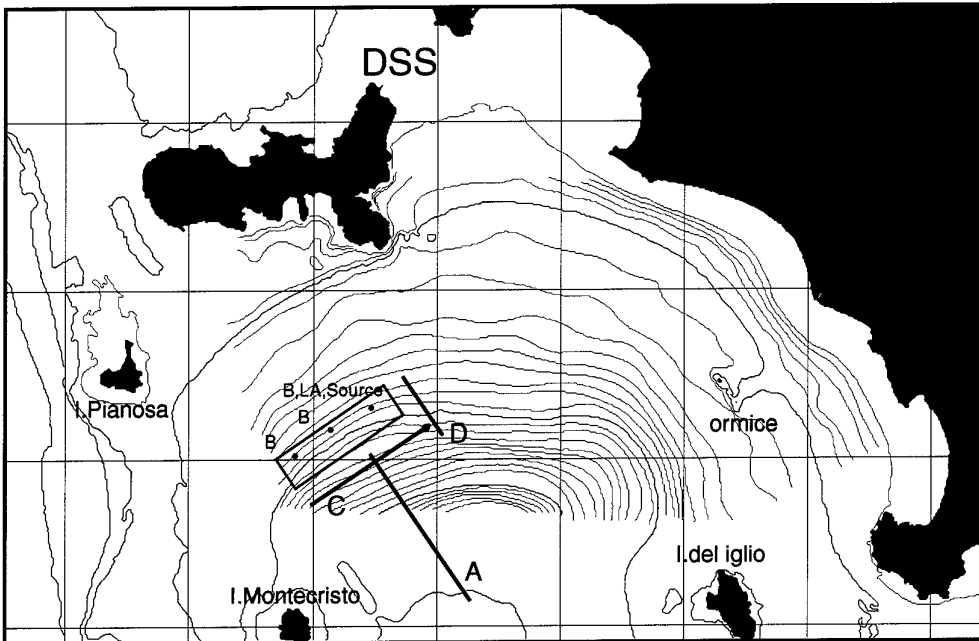


**Figure 1** Map of the DUSS field in DUSS'97 experiment. The source, monostatic receiver n.1, bistatic receivers n.2, n.3 are shown with target trajectories of types "A", "C", "D".

**3.1 Experimental data**

This section analyzes the contact localization precision obtained by the experimental DUSS system during the campaign "DUSS'97". Acoustic contacts from the three receivers are compared with DGPS data in a few significant runs performed with an Echo Repeater, with a large SNR (above 25 dB at sonar output for most echoes). Table 3 lists the processed runs and their characteristics, Fig. 2 shows an example of the positions of acoustic contacts from the three receivers on the geographical map, in three consecutive runs of different types.

**Table 3** Summary of runs.

RUN	Freq. kHz	Duration minutes	Source depth m	Target depth m	Target traj.
0103	3.5	90	110	90	C
0203	3.5	120	110	90	A
0104	3.5	60	110	90	D
0201	1.9	120	80	90	C

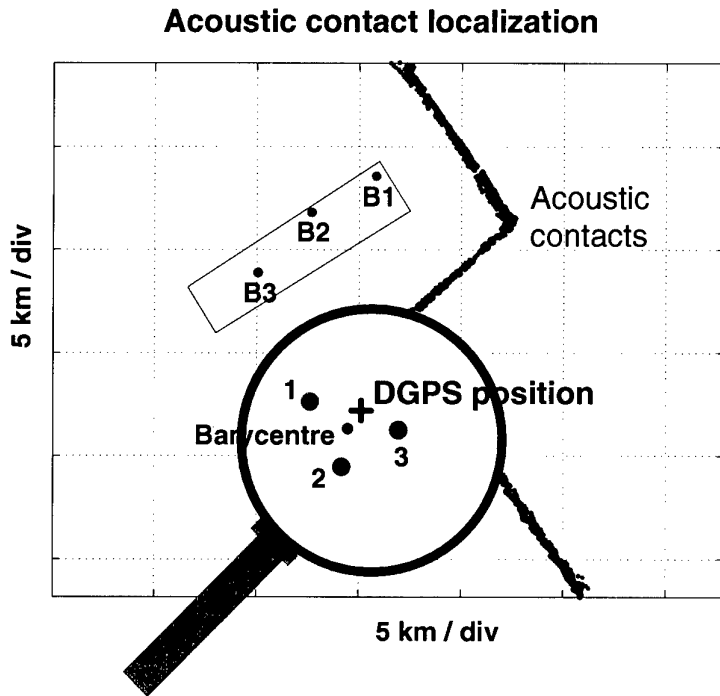


**Figure 2** Contact localization with three DUSS buoys versus DGPS target position.

In the following pictures, the displacement of each acoustic contact from the real DGPS target position (0; 0) is shown in a "scatter plot". The empirical distributions of range and bearing errors (relative to the receiver) are also shown. Figures 3, 4 show two significant examples of the processed data. Figures of all runs are in Annex B.

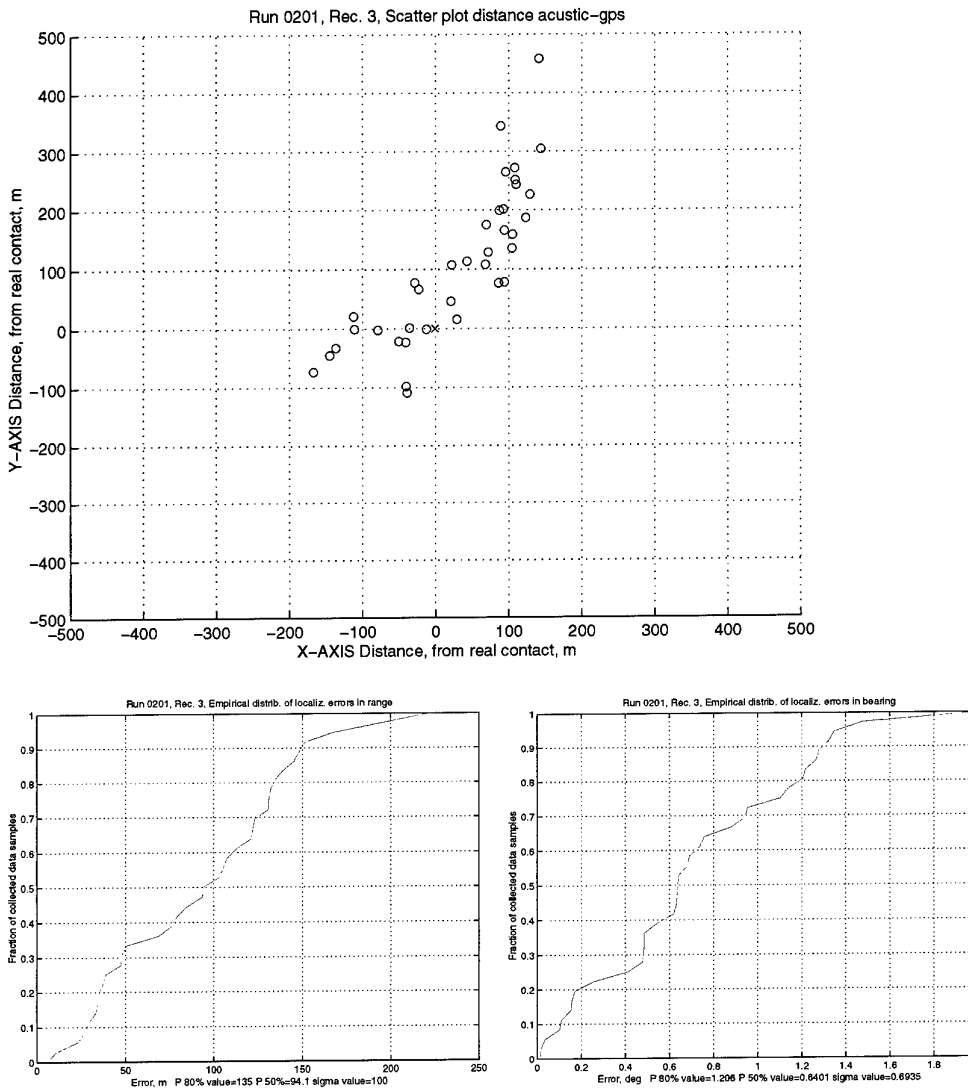


**Figure 3** RUN 0201, Receiver 3: scatter-plot of estimated echo location and empirical distributions of range and bearing errors.

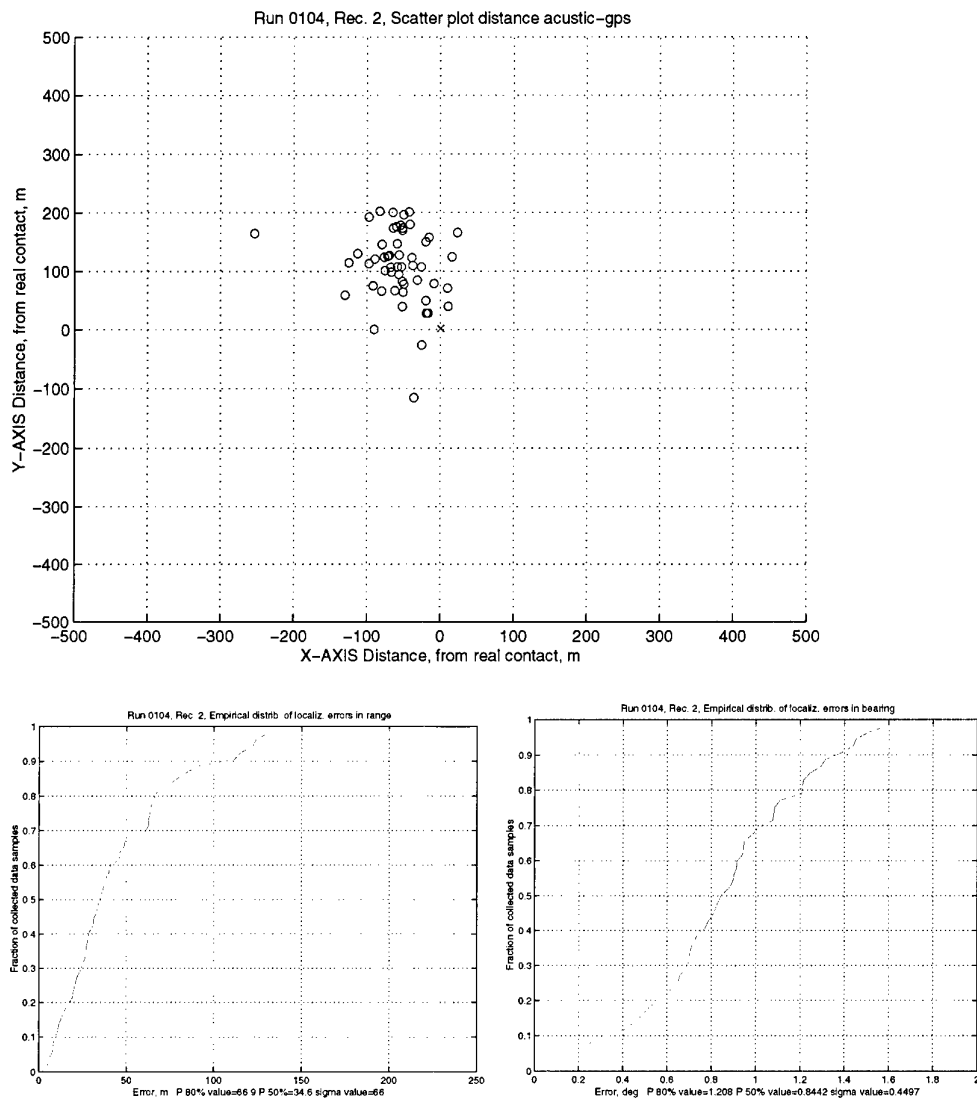


**Figure 4** RUN 0104, Receiver 2: scatter-plot of estimated echo location and empirical distributions of range and bearing errors.

### 3.2 Summary of results

Localization errors of acoustic contacts with respect to DGPS reference are expressed in terms of bearing and range from receiver. The tables below summarize measured range and bearing errors of echoes in terms of standard deviation and 80% percentiles. Mean errors are considered only in the range case.

**Table 4** Summary of localization range errors

RUN	Receiver 1 range errors (meters)			Receiver 2 range errors (meters)			Receiver 3 range errors (meters)			Freq. kHz
	$P_{0.8}$	$\mu_r$	$\sigma_r$	$P_{0.8}$	$\mu_r$	$\sigma_r$	$P_{0.8}$	$\mu_r$	$\sigma_r$	
0103	75	-33	49	92	35	67	105	37	77	3.5
0203	102	-60	42	77	-38	46	72	30	48	3.5
0104	106	-62	69	67	3	66	52	6	47	3.5
0201							135	40	100	1.9

Global averages are:

- $\langle \mu_r \rangle = 9.7 \text{ m}$
- $\sigma_r = 55 \text{ m}$

The global bias is averaged out from the whole set of collected data (all runs, all receivers). It is very close to zero. The bias of each individual run, on the other hand, is derived from a smaller set of pings, and is, on the average, 37 m. This fact leads to interpret localization errors as a random process with a slowly evolving component, which is uncorrelated between different runs, but correlated within each run. For that component, a run is a single sample, and errors don't average out. Such errors may derive from such effects as buoy drift, buoy location upon deployment, which represent an important component of DUSS characteristics.

This slowly – evolving variable term averages to zero on a large number of data points. Most range errors are within a  $P_{0.8}$  of 106 m.

**Table 5** Summary of localization bearing errors, degrees.

RUN	Receiver 1 bearing errors (deg)		Receiver 2 bearing errors (deg)		Receiver 3 bearing errors (deg)		Freq. kHz
	$P_{0.8}$	$\sigma_\theta$	$P_{0.8}$	$\sigma_\theta$	$P_{0.8}$	$\sigma_\theta$	
0103					1.0	0.6	3.5
0203	2.0	1.8	0.4	0.3	0.3	0.3	3.5
0104			1.2	0.5	0.9	0.3	3.5
0201					1.2	0.7	1.9

Bearing biases (i.e. mean errors) pertain to compass calibration and magnetic declination issues. Therefore they are not discussed here. Bearing variance (after calibration) is  $\sigma_\theta = 0.4^\circ$  globally and total bearing mean is near zero degrees ( $\mu_\theta = 0$ ). Some data from B<sub>1</sub> were omitted. In fact, it was hanging overboard NRV *Alliance*, and the pitching of the moored ship induced buoy rotations, which affected compass precision due to its slow response time. Also data from Run 0203 seem to be affected by such effects. All errors in the other cases are within  $P_{\theta_s} = 1.2^\circ$ .

The following Table 6 lists the statistics of global localization errors in the data set analyzed, for comparison with the tables above.

**Table 6** Summary of global localization errors.

RUN	Freq. kHz	Receiver 1 errors meters		Receiver 2 errors meters		Receiver 3 errors meters	
		$\mu_{LOC}$	$\sigma_{LOC}$	$\mu_{LOC}$	$\sigma_{LOC}$	$\mu_{LOC}$	$\sigma_{LOC}$
0103	3.5	194	212	92	54	120	84
0203	3.5	480	445	102	67	84	54
0104	3.5	213	176	134	54	156	60
0201	1.9					164	103

### 3.3 Discussion

The comparison with Cramer Rao bounds shows that  $\sigma_r$  is very large with respect to  $\sigma_{r\_CRAMER\_RAO}$  in all runs.

On the other hand,  $\sigma_\theta$  is very close to  $\sigma_{\theta\_CRAMER\_RAO}$ , as discussed also in the analysis of [4], Table 4, Pag. 13.

SNR values of the contacts are very large for most echoes [4]. Therefore the error contribution of noise interacting with pulse width and beam width is very limited in the present data set.

Other error factors therefore become evident: compass variance, buoy localization accuracy, mooring drift, pulse synchronization, estimation of  $c$  (velocity of sound) and acoustic path length in shallow water.

In the case of  $\sigma_r$ , these error factors become strongly visible in the experimental data set. In the case of  $\sigma_\theta$ , they are comparable to theoretical bounds. In both cases, the measurements are representative of these error factors, and effectively quantify them.

These factors and their individual contribution to overall performance are also discussed in [4]. Upon system design definition, improvements may be sought into the corresponding components. Wavefront distortion upon echo propagation is not discussed in the present analysis.

The real targets of an operational scenario produce barely detectable contacts, with low SNR. They are associated to negligible time / range errors but to large bearing errors ( $1^\circ - 2^\circ$ ) as shown in Tables 1, 2, Section 2. The corresponding contribution to localization errors would be predominant over the other system characteristics discussed so far (around 450 m at 20 km). Larger array apertures, with beams narrower than  $4^\circ$ , would produce errors around 250 m [4], consistent with the system potentials.

### 3.4 Conclusions

This section addresses the localization error performance of DUSS receivers when operated individually. The following results can be assumed as a reference in the next sections:

- $\langle \mu_r \rangle = 9.7$  m
- $\sigma_r = 55$  m
- $P_{0.8} = 106$  m.
- $\sigma_\theta = 0.4^\circ$
- $P_{0.8} = 1.2^\circ$

Monostatic and bistatic receivers do not show any noticeable differences in the available data set.

Range localization precision is satisfactory. The error contribution of limited SNR and peak width of the FM pulse (estimated by Cramer Rao lower bounds) is well below the present results, also for barely detectable contacts (Tab. 2). The present performance can therefore be maintained also with weak echoes, and depends mainly on the moorings and buoy localization precision. The partial bias  $\langle |\mu_r| \rangle = 37$  m indicates that some error factors, as buoy mooring drift and propagation time, fluctuate slowly in time, with a correlation constant more than 1 hour. The global bias  $\langle \mu_r \rangle = 9.7$  m is negligible. The error can be assumed as a zero mean random process of  $\sigma_r = 55$  m.

Bearing information, on the contrary, is responsible for the largest part of global localization errors. The error contribution of limited SNR and beam-width (estimated by Cramer Rao lower bounds) is negligible in the present data set, which is therefore representative of the typical technical constraints of DUSS. Compass variance, hydrophone frame rigidity, hydrophone phase response are the main system parameters

involved. Wavefront distortion is not discussed here. Upon real target detection, on the other hand, average SNR values will be much lower than in the present data set. The corresponding errors, estimated by Cramer Rao bounds, would still be negligible in range, but very large in bearing. A larger acoustic aperture is therefore required. As shown in [4], Table 8, page 18, an objective beam - width of  $4^\circ$ , corresponding to  $\sigma_{Loc} \leq 250 \text{ m}$  up to  $20 \text{ km}$ , can be assumed as the system specification for satisfactory target localization with a single receiver. The existing compass, offering a  $\sigma_\theta = 0.1^\circ$ , can be confirmed as a system specification.

For single-buoy localization of targets, priority should therefore be given to large array apertures. This parameter is critical for DUSS, in term of deployment, cost, processing overhead, receivers complexity, data transport.

A different localization concept is investigated in the following sections, resorting mainly to time information and taking advantage of the physical separation of small distributed receivers.

## 4

## Integrated target localization with multistatic active sonar: 2 receivers, time only

---

The advantages of a multistatic active sonar in target localization are shown in this section. Multiple, distributed receivers can be used in an integrated way for a more accurate localization of targets. Time – only localization (“Tri-lateration”) resorts to the intrinsic precision of time – of – arrival estimation shown above. It also involves limited array and processing complexity. This section addresses the case of two receiver buoys (a monostatic one, including the transmitter, plus a bistatic receiver). The effects of various system configurations and parameters on overall results are examined. The following sections address the effects of asymmetric time estimation precision on the two receivers, of receiver separation, of buoy localization precision, of acoustic path length and speed. Some receiver directivity is required to associate the contact pairs from the two receivers with each other and to permit / improve detection. Such directivity, though, does not affect localization precision results. On the other hand, it solves the ambiguity about target position above or below the buoys, visible in the maps below. The necessity and quantity of required receiver directivity is not studied here. The configuration with three buoys is addressed in Section 6; overall precision is improved by the contribution of three independent solutions (for the three pairs of buoys involved).

Models are implemented to determine target localization errors by means of Monte Carlo simulations. Input error statistics are derived from the experimental data analyzed above. Average localization errors are therefore computed.

### 4.1 Time-only localization with 2 receivers and 1 source.

The statistics of delay estimation errors collected in the previous section are used as a reference for simulations. The effects of such inputs on overall localization errors of the multistatic system are estimated via Monte Carlo simulations (See Annex A). A comparison is made with the classical single-buoy method. The standard deviation  $\sigma_\tau$  of time – of – arrival data in the experiments is summarized in the table below. Values range from 55 to 100 ms. The reference of  $\sigma_\tau=55$  ms is taken for receiver n.1 and  $\sigma_\tau=59$  ms for receiver n.2 from Run 0203. Although the global  $\sigma_r = 55$  m roughly corresponds to  $\sigma_\tau = 70$  ms, Run 0203 is assumed to represent the performance of a good operational DUSS.

**Table 7** Summary of mean and std values localization errors

RUN	Receiver 1 errors distance(ms)		Receiver 2 errors distance(ms)		Receiver 3 errors distance(ms)		Freq. kHz
	$\mu_\tau$	$\sigma_\tau$	$\mu_\tau$	$\sigma_\tau$	$\mu_\tau$	$\sigma_\tau$	
0103	-43	65	43	71	-3	70	3.5
0203	-80	55	-41	59	44	59	3.5
0104	-82	91	8	100	-6	75	3.5
0201					11	70	1.9

- $\mu_\tau$  is mostly representative of systematic errors in the estimation of acoustic path length and travel time, in the buoys positions, in system synchronization.
- $\sigma_\tau$  pertains to the variability of travel time from ping to ping, from environmental fluctuations and configuration geometry changes.

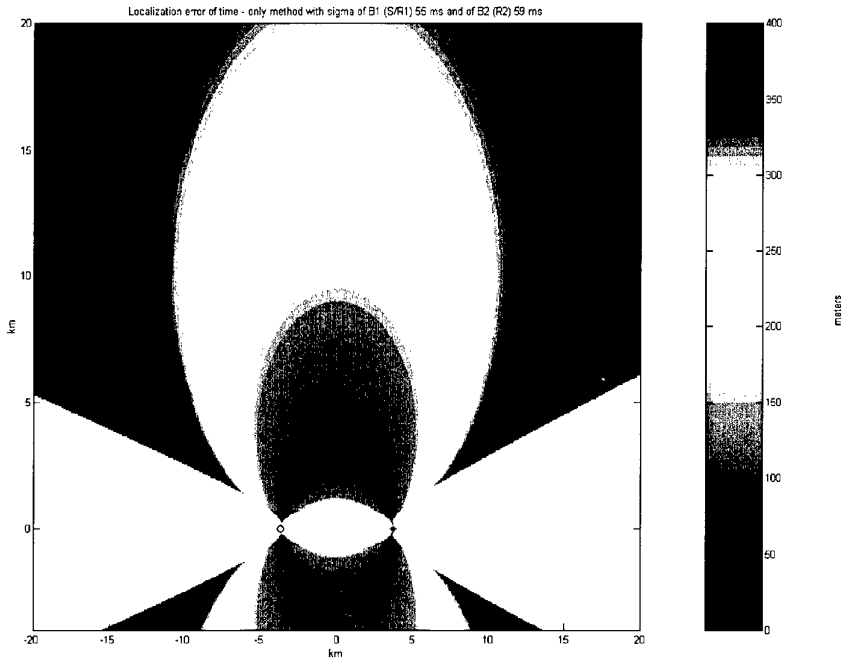


**Figure 5** Localization error of time – only localization method with two buoys only, 4 n.mi apart ( $\sigma_{\tau_1}=55\text{ ms}$   $\sigma_{\tau_2}=59\text{ ms}$ ).

Figure 5 represents the geographical map of the sonar surveillance area. The source/receiver n.1 (left) are represented with a circle and the receiver n.2 is represented with a star. The Monte Carlo simulation estimates the mean localization errors with a colour scale for each potential target position. All simulations are obtained with 25 iterations in the colour plots, 5000 iterations in the tables below. The standard deviation of the estimation is 1/25 or 1/5000 of the estimated mean for each target position [10]. The white zones indicate that during the simulation, no solution existed for at least one iteration. These critical areas require additional inputs for target localization (e.g. an additional receiver, like in the tri-lateration method).

The lower part of the map is symmetrical, due to localization ambiguities that the use of three buoys (tri-lateration) eliminates. Errors increase with distance, and are minimum in front of the two buoys.

**Table 8** Summary of positioning error values from Fig. 5. The relationship is roughly linear.

Position of target km		Mean error (meters) $\sigma_x=55$ ms $\sigma_y=59$ ms
X	Y	
0	5	98
0	10	150
0	15	210
0	20	270

Mean errors are limited to 100 m (at 5 km), 150 m (at 10 km), and 210 m (at 15 km). The light blue area in Fig. 5 therefore indicates the limits where DUSS with time-only localization offers excellent results.

#### 4.1.1 Model validation with real data.

The time only localization method has been applied to real data from Run 0103. Simulated data use the specific statistics computed for Run 0103 (Table 7). Table 9 below summarizes the results and compares them to single – buoy localization.

**Table 9** Summary of global localization errors.

RUN	Freq. kHz	Receiver 1 errors [meters]		Receiver 3 errors [meters]		Time-only localization method real data [meters]		Time-only localization method simulation [meters]	
		$\mu_{LOC}$	$\sigma_{LOC}$	$\mu_{LOC}$	$\sigma_{LOC}$	$\mu_{LOC}$	$\sigma_{LOC}$	$\mu_{LOC}$	$\sigma_{LOC}$
0103	3.5	194	212	120	168	194	84	157	110

The real data successfully confirm localization results from the model.

#### 4.2 Influence of system parameters on time-only localization

The present section estimates the effects on overall precision of the following system parameters: time estimation variance of the monostatic / bistatic buoys, buoys separation, buoy localization precision, acoustic path speed and length. Indications about system design tradeoffs are drawn.

##### 4.2.1 Different precision of monostatic and bistatic buoy.

The following two figures and table 10 show the effect of asymmetric  $\sigma_r$  values for the monostatic and bistatic units of the pair.

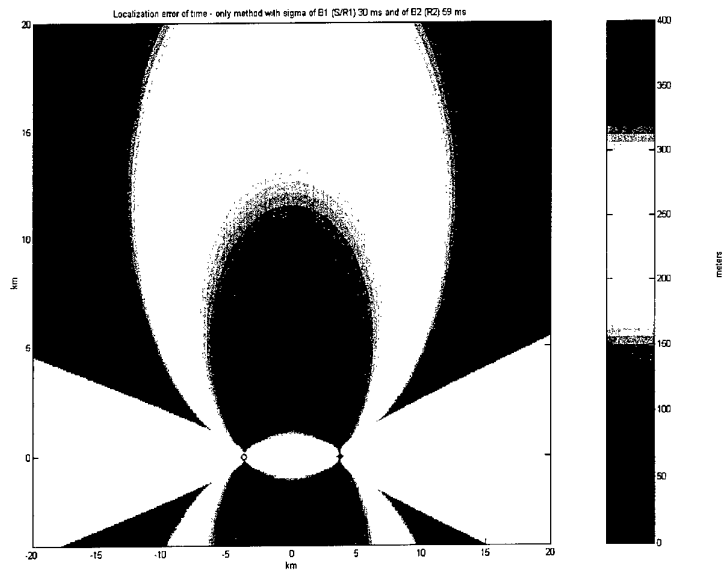


**Figure 6** Localization error of time - only method with two buoys only ( $\sigma_{\tau_1}=30$  ms  $\sigma_{\tau_2}=59$  ms).

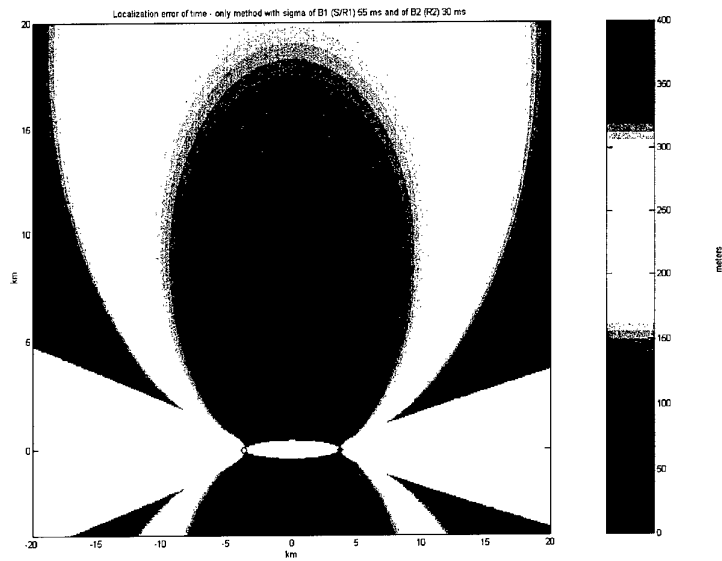


**Figure 7** Localization error of time - only method with two buoys only ( $\sigma_{\tau_1}=55$  ms  $\sigma_{\tau_2}=30$  ms).

**Table 10** Summary of the results.

Position of target km		Case 1 – (meters) $\sigma_{t_1}=55$ ms $\sigma_{t_2}=59$ ms	Case 2 – (meters) $\sigma_{t_1}=30$ ms $\sigma_{t_2}=59$ ms	Case 3 – (meters) $\sigma_{t_1}=55$ ms $\sigma_{t_2}=30$ ms
X	Y			
0	5	98	84	71
0	10	150	124	114
0	15	210	173	162
0	20	270	225	211

The monostatic and bi-static receivers behave nearly in the same way. Time errors are slightly more critical on bi-static units (10 %) at all target ranges beyond 5 km.

**4.2.2 Influence of sensors separation**

Increasing the distance between the two sensors (as shown in Fig. 8) the localization error is reduced.

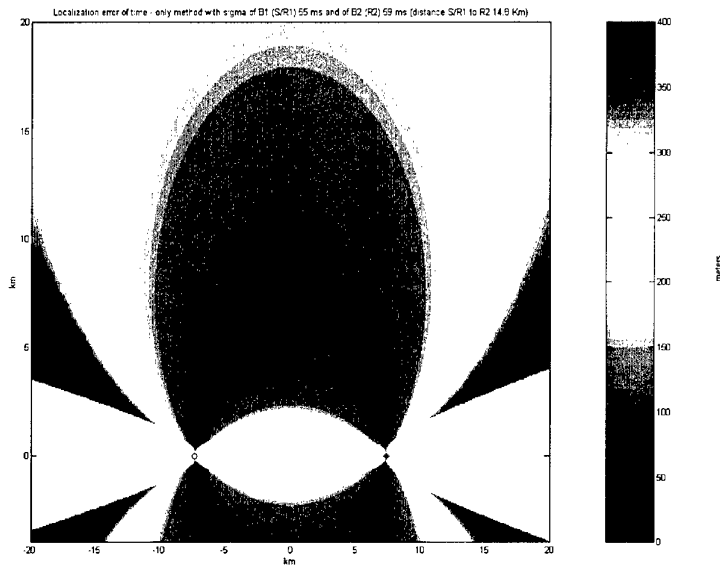


**Figure 8** Localization error of time - only method with increased separation between two buoys (8 n.mi,  $\sigma_{t_1}=55$  ms  $\sigma_{t_2}=59$  ms, same as Fig. 5).

The following table 11 shows remarkable reductions of localization errors (39 % - 45 % doubling the distance).

**Table 11** Summary of positioning errors for different sensor separation ( $\sigma_{t_1}=55$  ms  $\sigma_{t_2}=59$  ms).

Position of target km		Case 1 distance 4 miles (7.4 km)	Case 1 distance 6 miles (11.1 km)	Case 3 distance 8 miles (14.8 km)
X	Y			
0	5	98	89	92
0	10	150	111	97
0	15	210	146	120
0	20	270	185	149

The only exception takes place at very short target ranges. A separation of 8 miles is recommended to fully take advantage of the time – only localization method.

**4.2.3 Influence of buoy localization precision**

The effects of receiver localization precision on target position estimation are modelled here (Fig.9). Several  $\sigma_{pos}$  hypotheses are assumed here. Table 12 summarizes the results. Errors are roughly linear with  $\sigma_{pos}$ .

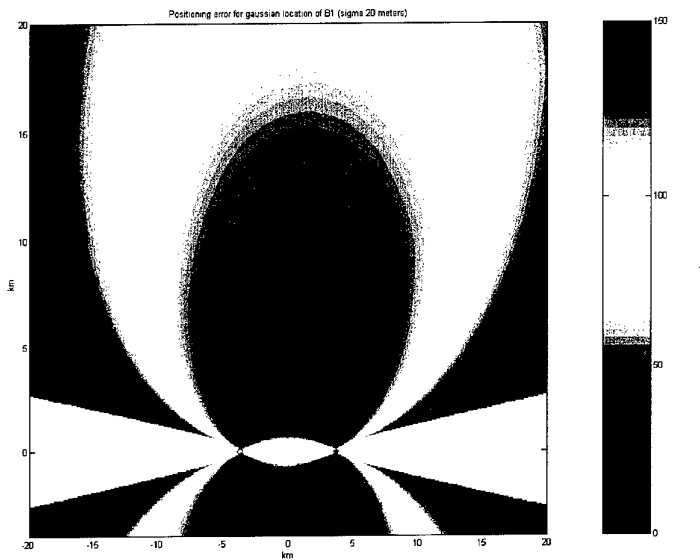


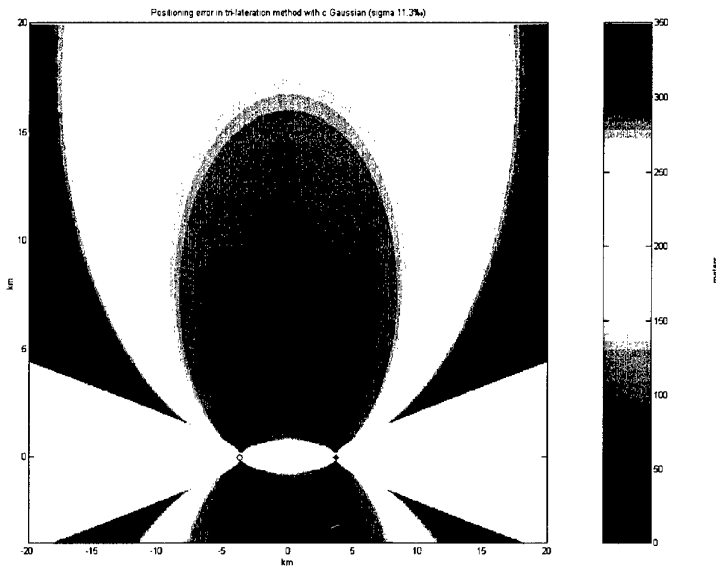
**Figure 9** Localization error of time - only method with two buoys only with wrong buoy position ( $\sigma_{pos}$  20 m). Note: the error scale is 0 – 150 m.

**Table 12** Summary of localization errors for different buoy positioning error values in time –only method.

Position of target Km		Localization error (meters)	Localization error (meters)	Localization error (meters)
X	Y	$\sigma_{pos}=10$ m	$\sigma_{pos}=20$ m	$\sigma_{pos}=40$ m
0	5	13	25	51
0	10	19	37	76
0	15	27	52	106
0	20	34	67	137

**4.2.4 Influence of acoustic path length and travel time**

Accurate estimations of the length and travel times of acoustic paths connecting buoys to targets are very critical for the localization of contacts. A brief analysis was carried out [5] to estimate worst - case errors that can be made when acoustic paths are not modelled at all, using target distance and average sound speed instead. The maximum estimated error corresponds to 11 ‰ of sound speed. Figure 10 shows the corresponding localization errors computed by the simulation.



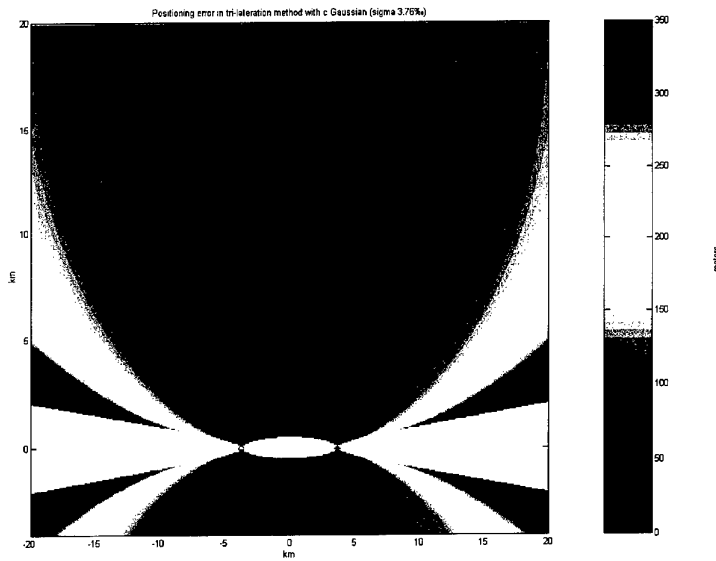
**Figure 10** Localization errors of time –only method ( $\sigma_c = 11$  ‰ of  $c$ ). Note: the error scale is 0 – 350 m.

Table 13 below summarizes the results.

**Table 13** Summary of simulated localization errors of time-only method. The effect of  $\sigma_c = 11 \text{ ‰}$  is compared with the effects of the measured global  $\sigma_r$  with the Monte-Carlo simulation.

Position of target km		Error from $\sigma_c$	Error from measured global $\sigma_r$	Relative error
X	Y			
0	10	100 m	150 m	67 %
0	20	185 m	270 m	69 %

The exact knowledge of SVP in 3-D bistatic scenario, of the bottom structure and the precision of the corresponding propagation simulations produce lesser effects. Such effects correspond to 4‰ of the sound speed [8]. The resulting localization errors (with time-only localization) are simulated in Fig. 11.



**Figure 11** Localization error of time-only method ( $\sigma_c = 4 \text{ ‰}$  of  $c$ ).

Table 14 below summarizes the results.

**Table 14** Summary of simulated localization errors of time-only method. The effect of  $\sigma_c = 4\%$  is compared with the effects of the measured global  $\sigma_r$  with the Monte-Carlo simulation.

Position of target km		Error from $\sigma_c$	Error from measured global $\sigma_r$	Relative error
X	Y			
0	10	30 m	150 m	20 %
0	20	60 m	270 m	22 %

The accuracy of modelling is therefore a second – order problem. It still represents a very important parameter for system design, when performance improvements are sought. This issue, in fact, does not impact on the cost or complexity of the deployed systems, and does not represent a heavy computational load for a multistatic sonar processor. This section therefore proves the importance of modelling, particularly in heavy range-dependent environments, where the acoustic paths to the buoys may differ substantially from each other.

**4.3 Comparison of time-only, 2 receivers vs time-and-bearing, 1 receiver.**

Table 15 compares the time-only, 2 buoys case with single-buoy localization errors (from both bearing and time information). As explained in 5.1 below,  $\sigma_\theta=0.7^\circ$  was chosen as a reference for typical DUSS receiver performance requirements when directivity is relevant for localization. It corresponds to  $4^\circ$  wide beams with barely detectable targets (Equation 2.1). Therefore the receivers involved in this comparison are not necessarily equivalent. While the single-buoy case requires a good directivity, the time-only, two-buoys method is not directly affected by it, although resorts to it for contact detection association.

**Table 15** Comparison of single-buoy time-and-bearing localization with time - only localization method.

Position of target km		Receiver n.1 Time + bearings Localization error (meters) $\sigma_r=55$ ms $\sigma_\theta=0.7^\circ$	Receiver n.3 Time + bearings Localization error (meters) $\sigma_r=59$ ms $\sigma_\theta=0.7^\circ$	Two buoys Time only Localization error (meters) $\sigma_r=55$ ms $\sigma_\theta=59$ ms 8 n.mi separation	Two buoys Time only Localization error (meters) $\sigma_r=55$ ms $\sigma_\theta=59$ ms 4 n.mi separation
X	Y				
0	5	100	125	92	98
0	10	133	153	97	150
0	15	174	192	120	210
0	20	218	232	149	270

# 5

## Integrated target localization with multistatic passive sonar: 2 receivers

---

This section examines localization precision of a pair of passive deployable receivers. Bearings – only localization (“Tri-angulation”) requires more complex receivers, with large apertures and directivity, but is particularly interesting for passive surveillance. Time-only localization of an Autonomous Underwater Vehicle (AUV) provided with an FM synchronous pinger is also considered. The effects of various system configurations and parameters on overall results are examined. The following sections address the effects of asymmetric errors on the two receivers, of receiver separation, of buoy localization precision, of acoustic path length and speed. The AUV case, like the active sonar case of Section 5, requires some receiver directivity to associate the contact pairs from the two receivers with each other and to improve detection. Such directivity, though, does not affect localization precision, but it solves the ambiguity about target position above or below the buoys, visible in the maps below. The case with three buoys is addressed in Section 6; overall precision is improved by the contribution of three solutions (for the three pairs of buoys involved).

Models are implemented to determine target localization errors by means of Monte Carlo simulations. Annex A, Section A.2 describes the details. Input error statistics are derived from the experimental data analyzed above. Average localization errors are therefore computed.

### 5.1 Tri-angulation localization system

Several values of  $\sigma_\theta$  are considered in the simulations (from  $0.25^\circ$  to  $1^\circ$ ). Figures 12 and 13 and Table 17 summarize the results. The reference value of  $\sigma_\theta = 0.7^\circ$  corresponds to  $4^\circ$  wide beams (Eq. 2.1), with barely detectable targets. At the same time, it is consistent with the experimental measurements, which, as discussed above, are representative of the typical characteristics of the experimental DUSS.

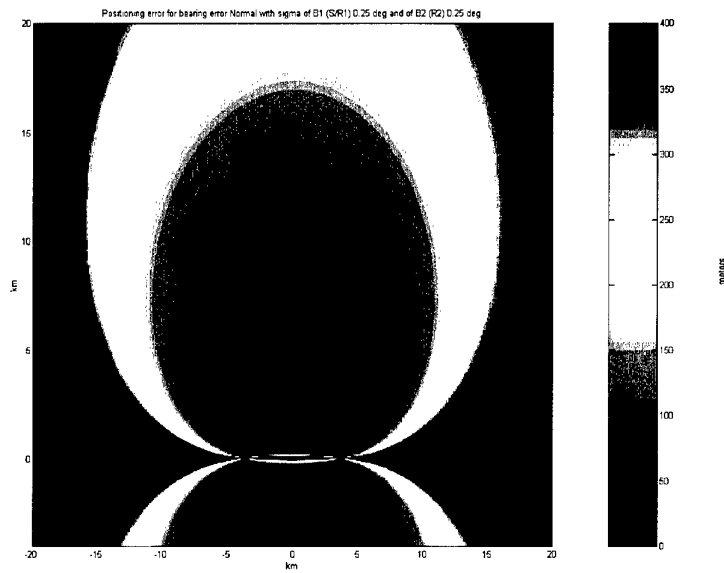


**Figure 12** Localization error in triangulation method ( $\sigma_{\theta_1}=0.25^\circ$   $\sigma_{\theta_2}=0.25^\circ$ ). The error scale is 0 – 400 m.

The best performance is obtained in the area in front of the two buoys. As shown by Table 17, mean errors below 250 m can be obtained up to 10 km ranges with  $\sigma_\theta = 0.7^\circ$ .

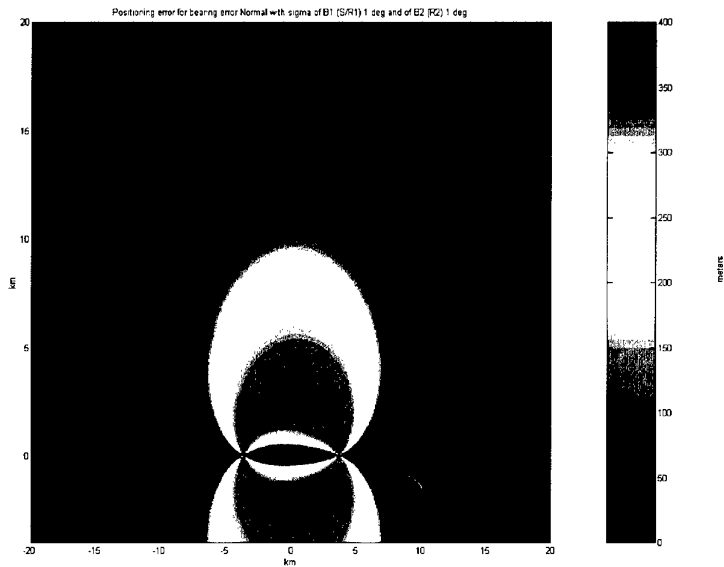


**Figure 13** Localization error in triangulation method ( $\sigma_{\theta_1}=1^\circ$  ,  $\sigma_{\theta_2}=1^\circ$ ). The error scale is 0 – 400 m.

**Table 17** Summary of mean localization errors with tri-angulation localization method. Buoy separation is 4 n.mi, like in the experiments.

Position of target km		Case 1 $\sigma_{\theta_1}=0.25^\circ$ $\sigma_{\theta_2}=0.25^\circ$	Case 2 $\sigma_{\theta_1}=0.4^\circ$ $\sigma_{\theta_2}=0.4^\circ$	Case 3 $\sigma_{\theta_1}=0.7^\circ$ $\sigma_{\theta_2}=0.7^\circ$	Case 4 $\sigma_{\theta_1}=1^\circ$ $\sigma_{\theta_2}=1^\circ$
X	Y				
0	5	36	56	99	143
0	10	86	137	241	350
0	15	172	272	479	698
0	20	289	461	811	1188

**5.1.1** Dependence on system parameters.

The present section estimates the effects on overall precision of such system parameters as buoys separation and localization precision. Buoy – to - buoy separation is considered, comparing a 6 n.mi separation to the 4 n.mi reference of the experimental DUSS configuration. Improvements range between 16 % (at 10 km) and 40 % of total errors (at 20 km).

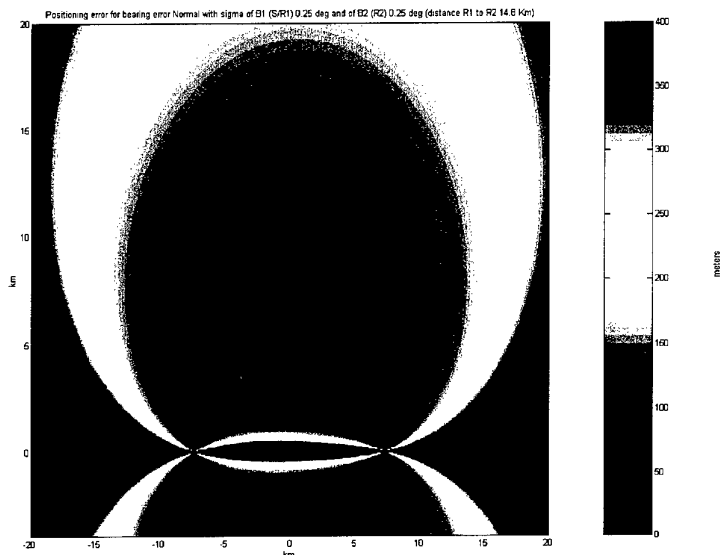


**Figure 14** Localization errors of tri-angulation method with increased separation between the two buoys (6 n.mi,  $\sigma_{\theta_1}=0.25^\circ$ ,  $\sigma_{\theta_2}=0.25^\circ$ , same as Fig. 12).

**Table 17** Summary of localization errors for different buoy separation and  $\sigma_\theta$  values.

Position of target km		Case 1 distance 4 miles (7.4 km) $\sigma_{\theta_1}=0.25^\circ$ $\sigma_{\theta_2}=0.25^\circ$	Case 2 distance 6 miles (11.1 km) $\sigma_{\theta_1}=0.25^\circ$ $\sigma_{\theta_2}=0.25^\circ$	Case 3 distance 4 miles (7.4 km) $\sigma_{\theta_1}=0.7^\circ$ $\sigma_{\theta_2}=0.7^\circ$	Case 4 distance 6 miles (11.1 km) $\sigma_{\theta_1}=0.7^\circ$ $\sigma_{\theta_2}=0.7^\circ$
X	Y				
0	5	36	52	99	146
0	10	86	72	241	198
0	15	172	114	479	314
0	20	289	174	811	480

The “tri-angulation” method is robust to buoy localization errors (Fig. 15 and table 19). A  $\sigma_{pos} = 20$  m contributes, alone, to 16 % of errors at 10 n.mi and to 8 % at 20 km. Therefore, system specifications and constraints are determined by the requirements of the time – only case.

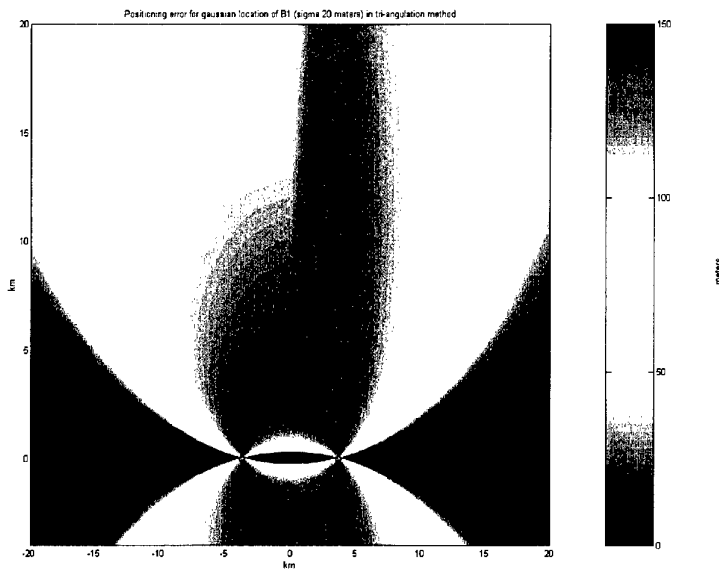


**Figure 15** Localization errors of tri-angulation as a function of localization errors on one receiver ( $\sigma_{pos} = 20$  m). Buoy separation is 4n.mi.

**Table 19** Summary of localization errors with errors on buoy position ( $\sigma_{pos} = 20$  m). Buoy separation is 4 n.mi.

Position of target Km		Mean error [meters] $\sigma_{pos}=20$ m
X	Y	
0	5	27
0	10	38
0	15	52
0	20	68
3.7	10	23
3.7	15	26
3.7	20	29

**5.2 Time-only localization of AUV with 2 receivers.**

An autonomous underwater vehicle (AUV) with an active pinger transmitting synchronized LFM pulses is considered here. The model (presented in Annex A, section A.1.2) determines mean localization errors with Monte Carlo simulations. Results are presented in Fig. 16 and Table 20. Input errors  $\sigma_{\tau_1}=55$  ms and  $\sigma_{\tau_2}=30$  ms are considered. The latter value assumes more precise time – of – arrival estimations than in the echo repeater experiments, since acoustic paths are one-way only.

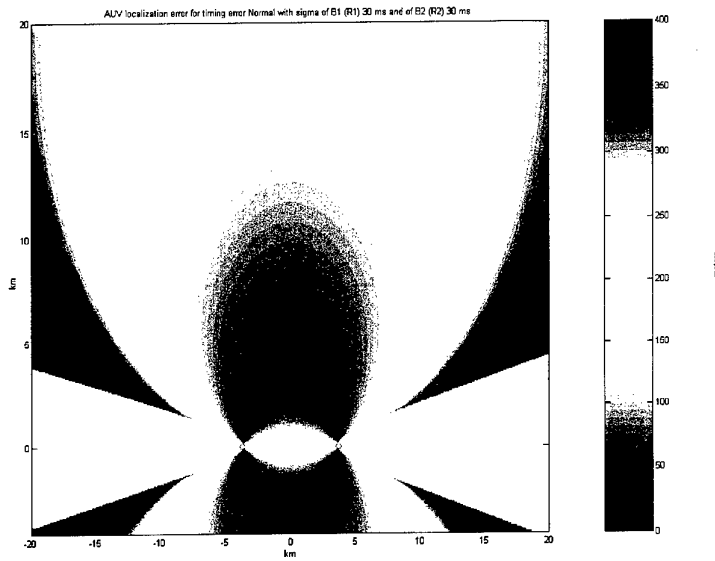


**Figure 16** AUV localization error with DUSS ( $\sigma_{\tau_1}=30$  ms  $\sigma_{\tau_2}=30$  ms). Buoy separation is 4 n.mi. The error scale is 0 – 400 m.

**Table 20** Summary of AUV localization errors with DUSS method.

Position of target Km		Mean error [meters]	Mean error [meters]
X	Y	$\sigma_{r_1}=30$ ms $\sigma_{r_2}=30$ ms	$\sigma_{r_1}=55$ ms $\sigma_{r_2}=55$ ms
0	5	59	108
0	10	83	152
0	15	114	208
0	20	146	268

Satisfactory results of 146 m at 20 km can be achieved.

### 5.3 Conclusions

The present overview of multistatic passive and AUV target localization methods, using one pair of sensors, provides the following error estimates. Localization errors span a wide range of values, according to target position. The plots clearly indicate the blue area in front of the buoys where performance is best, also at relatively long ranges. Summary results are referred to discrete points in that area. More buoys need to be deployed to extend the "precise" area further.

Passive bearings- only localization is subject to errors of 241 m at 10 km.

AUV time - only localization is subject to errors of 83 m at 10 km.

Inter sensor separation is the most critical parameter. An increase from 4 to 6 n.mi for passive operation is recommended.

Buoy localization needs to be accurate within 20 m.

The use of propagation modelling to compute travel time is also very critical (In the AUV case only). Very accurate environmental assessment can also contribute, to a lesser extent, to overall system precision.

Beam widths of 4° are recommended for passive, bearings – only operation. This involves receiver apertures larger than the existing system.

## 6

## Target localization with three sensors

The use of three sensors (one monostatic source/receiver and two receivers) for multistatic, time-only target localization increases precision in the surveillance area common to all receivers. The present section addresses the cases of active sonar ("Tri-lateration") and of AUV pinger localization.

### 6.1 Time-only localization: tri - lateration

Monte Carlo simulations estimate mean localization errors of the tri-lateration method starting from  $\sigma_r$  values measured in the experiments. Annex A, Section A.3 describes the details. Figures visualize the results for each potential target position on the geographical map with a colour scale just like in the previous section (Fig. 17).

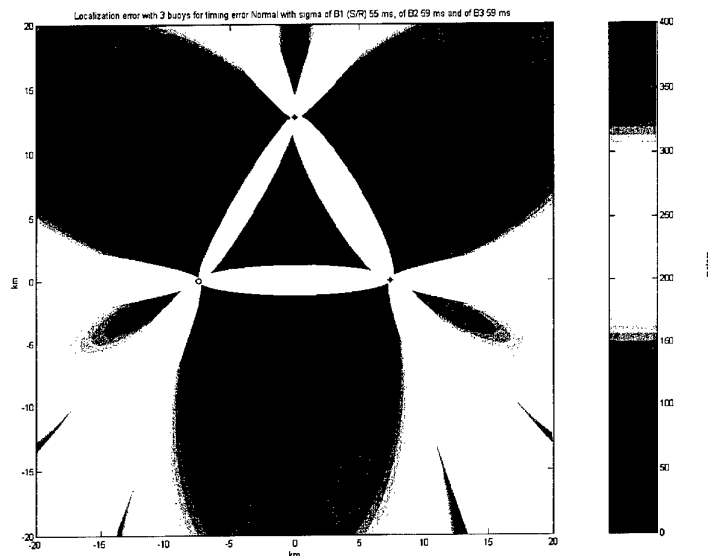


**Figure 17** Localization error of time - only method with three buoys ( $\sigma_{r_1}=55$  ms  $\sigma_{r_2}, \sigma_{r_3}=69$  ms). Buoy separation is 8 n.mi. The map scale is 40 km x 40 km. The error scale is 0 – 400 m.

The source/receiver n.1 are represented in the figures below with a circle and the receivers n.2 and n.3 is represented with a star. The white areas correspond to a reduced solution, obtained only from two pairs of buoys instead than three.

All simulations are obtained with 25 iterations in the colour plots, 5000 iterations in the data of the following tables. The standard deviation of the estimation is 1/25 or 1/5000 of the estimated value for each target position [10].

The maps clearly show the blue areas inside the bye triangle and immediately outside it, in front of its sides, where performance is best.

**Table 21** Summary of localization error values from Fig. 17.

Position of target Km		Mean error [meters] ( $\sigma_{r_1}=55$ ms $\sigma_{r_2}=59$ ms $\sigma_{r_3}=59$ ms)
X	Y	
0	4.3	89
-15	10	115

The error is minimum in the centre of three buoys and localization is more precise than with two buoys only. Table 22 shows that error reductions range between 8 % and 42 %.

**Table 22** Comparison between tri-lateration localization methods with two buoys and with three buoys.

Position of target Km		Error with time-only localization method with three buoys* [meters]	Error with time-only localization method with two buoys** [meters]	Gain (%)
X	Y			
0	4.3	89	97	8%
-15	10	115	200	42%

Value of std parameters used in simulation  
 \*  $\sigma_{r_1}=55$  ms  $\sigma_{r_2}=59$  ms  $\sigma_{r_3}=59$  ms  
 \*\*  $\sigma_{r_1}=55$  ms  $\sigma_{r_2}=59$  ms

**6.2 AUV time –only localization**

An Autonomous Underwater Vehicle (AUV) with a synchronized FM pinger is localized by three receivers using only time – of – arrival information. Monte Carlo simulations estimate mean localization errors starting from  $\sigma_r = 30$  ms. This value is derived from the experiments, on the assumption that one-way paths are related to half the measured errors. Annex A, Section A.3 describes the details. Figure 18 visualizes the results for each potential target position on the geographical map with a colour scale as in the previous section.

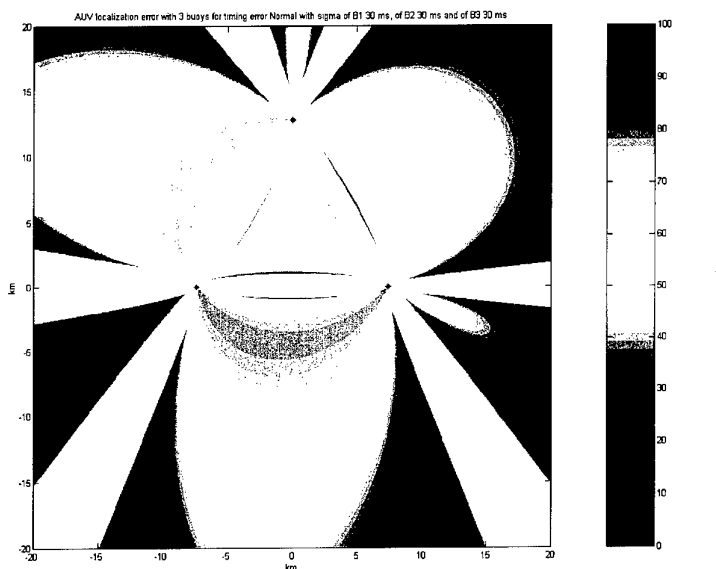


**Figure 18** AUV localization error with DUSS using three buoys ( $\sigma_{\tau_1}=30$  ms  $\sigma_{\tau_2}=30$  ms  $\sigma_{\tau_3}=30$  ms). The map scale is 40 km x 40 km. The error scale is 0 – 100 m. The distance between buoys is 8 n.mi.

**Table 23** AUV localization errors with DUSS from Fig. 18.

Position of target Km		Mean error [meters]
X	Y	( $\sigma_{\tau_1}=30$ ms $\sigma_{\tau_2}=30$ ms $\sigma_{\tau_3}=30$ ms)
0	4.3	46
-15	10	60

The best performance is obtained in the centre of the triangle.

**Table 24** Comparison between AUV localization methods with two buoys and with three buoys.

Position of target Km		Mean error of AUV method with two buoys*	Mean error with AUV localization method with three** buoys [meters]	Gain (%)
X	Y	[meters]		
0	4.3	65	46	29%
-15	10	110	60	45%

\*  $\sigma_{\tau_1}=30$  ms  $\sigma_{\tau_2}=30$  ms  
 \*\*  $\sigma_{\tau_1}=30$  ms  $\sigma_{\tau_2}=30$  ms  $\sigma_{\tau_3}=30$  ms

*6.3 Conclusions*

The method with three buoys reduces localization errors by 30 – 45 %. In fact each point is computed from three solutions of the 2 – buoy method. The ambiguities observed with one pair of buoys only are also eliminated.

## 7

## Conclusions and recommendations

---

The present document reports the results of target localization precision measurements taken in "DUSS'97" tests with an experimental DUSS (Deployable Underwater Surveillance System) and an Echo Repeater. This kind of target provides a differential GPS reference and strong Signal to Noise Ratios (SNR). Errors of time – of – arrival estimation range from 55 ms to 100 ms (both bias and standard deviation). Errors in bearings estimation range from  $0.3^\circ$  to  $0.6^\circ$ . These results are not affected by the interactions of limited SNR with pulse – width and beam – width, estimated by Cramer Rao Lower Bounds. Therefore they are representative of the peculiar system characteristics of a distributed network of multistatic sonar nodes. Time – of – arrival information is simpler to obtain, more robust to noise and produce in the DUSS experiments smaller localization errors than bearings information. Detection performance and system design issues are addressed in previous reports. A specification of  $4^\circ$  beams is expressed for bearings localization of weak targets. The existing compass precision of  $0.1^\circ$  is confirmed. This keeps performance compatible with DUSS characteristics.

The present measurements are used as a reference input to study the localization performance that can be obtained by DUSS using time – only and bearings – only multistatic localization methods. The large separation between the buoys improves target localization. The correct association of contacts from different buoys is not discussed here. Its feasibility has been demonstrated in Ref [4]. Monte Carlo simulations estimate localization errors for any target position. Colour maps and tables summarize the results. Results are validated by comparison with real data. Localization precision spans a wide range of values, according to target position. It is best around the symmetry axis passing between the buoys, also at relatively long ranges. Summary results are referred to discrete points in that area.

Methods using just **one pair of buoys** are considered first. This simplified case better shows the dependence of results on such system parameters as compass accuracy, buoy localization precision (for mono or multistatic units), inter – buoy separation, acoustic path travel time.

- **Time – only, active sonar:** an error better than 150 m is obtained at 10 km, 270 m at 20 km. This method achieves important performance improvements versus classical time – and – bearing localization with a single receiver (66 % of the errors) with wide inter – receivers spacing (8 n.mi) With only 4 n.mi spacing, performance is comparable up to ranges of 10 km, 20 % worse at 20 km..

- Sensor separation is very critical (39 % - 45 % error reduction passing from 4 to 8 n.mi). A distance of 8 n.mi at least is therefore recommended.

Buoy localization precision is also very important. A  $\sigma_{pos}$  of 20 m contributes, alone, to 25 % of total measured errors. In – buoy DGPS and corrections of the drift between the surface and submerged unit is therefore recommended.

The precision of bi-static buoys is slightly more critical than monostatic buoys precision (10 %).

Lack of propagation modelling to estimate acoustic travel time produces, alone, errors up to 70 % of the total measured errors. Lack of accuracy in modelling produces errors up to 20 % of measured errors.

- **Time – only, localization of AUV** (Autonomous Underwater Vehicle) with a synchronized FM pinger: average errors are 83 m at 10 km.
- **Passive bearings - only localization**: average errors of 250 m can be obtained up to 10 km ranges with  $\sigma_{\theta}=0.7^{\circ}$ , i.e. with beams of  $4^{\circ}$  and weak targets.

Inter sensor separation: passing from 4 n.mi to 6 n.mi, localization errors decrease by 16 % of total errors (at 10 km) and by 40 % (at 20 km).

Buoy localization errors:  $\sigma_{pos} = 20$  m contributes, alone, to 16 % of global errors at 10 n.mi and to 8 % at 20 km.

Beam widths of  $4^{\circ}$  are recommended for passive, bearings – only operation. This would be consistent with the intrinsic, measured bearings errors of the DUSS system.

The same estimations are extended to the case where time – only methods use **three receivers**. Better precision and coverage are obtained, while residual ambiguities are solved. Maximum error reductions of 45 % are demonstrated.

Further work about performance achievable in conjunction with target tracking and contact fusion algorithms is recommended, in order to proceed towards a complete assessment of operational potentials of DUSS.

## 8

## References

- 
- [1] Mozzone, L., Bongi, S. Deployable Underwater Surveillance Systems - analysis of experimental results. SACLANTCEN SR-278. La Spezia, Italy, NATO SACLANT Undersea Research Centre, 1997.
- [2] Mozzone, L., Bongi, S., Primo, F., Deployable Underwater Surveillance Systems - analysis of experimental results. Part II. SACLANTCEN SR-283. La Spezia, Italy, NATO SACLANT Undersea Research Centre, 1998.
- [3] Mozzone, L., Bongi, S. Deployable Underwater Surveillance Systems - analysis of experimental results. Part III. SACLANTCEN SR-288. La Spezia, Italy, NATO SACLANT Undersea Research Centre, 1998.
- [4] Mozzone, L., Bongi, S. Deployable Underwater Surveillance Systems - Deployable Underwater Surveillance Systems. Localization and fusion of multistatic contacts. Evaluation of feasibility using experimental data. SACLANTCEN SR-291. La Spezia, Italy, NATO SACLANT Undersea Research Centre, 1998.
- [5] Private discussion with Ferla, M. in APR 99.
- [6] Burdic, W. Underwater acoustic system analysis, Prentice-Hall., 1991: Paragraph 13.3.3. [ISBN 0-13-947607-5].
- [7] Installation and operation manual for model 3009/3012 differential GPS receiver. Del Norte technology Inc.
- [8] Nielsen, R. O. Sonar signal processing, Artech House, 1991, Paragraph 5.2.3 [ISBN 0-89006-453-9]
- [9] Papoulis, A. Probability, Random variables and stochastic processes, McGraw - Hill, 1991. Paragraph 4.2. [ISBN 0-07-048477-5].
- [10] Bendat, J.S., Piersol, A.G., Random data, analysis and measurement procedures, Wiley, 1971, ISBN: 0-471-06470-X.
- [11] Mozzone, L., Bongi, S. Diversity in deployable underwater surveillance systems. SACLANTCEN Report SR-318. La Spezia, Italy, NATO SACLANT Undersea Research Centre, 1999.
- [12] Mozzone, L., Bongi, S. Localization and fusion of echoes with deployable multistatic active sonar: evaluation of feasibility using experimental data. ECUA'98 Fourth European Conference on Underwater Acoustics, Roma, 1998.
- [13] Mozzone, L., Bongi, S. Diversity in multistatic active sonar, IEEE Oceans '99 Conference, 1999, Seattle, US.
- [14] Mozzone, L., Filocca, F., Bongi, S., Diversity in DUSS (Deployable Underwater Surveillance Systems) with CW pulses. SACLANTCEN Report SR-308. La Spezia, Italy, NATO SACLANT Undersea Research Centre, 1999.
- [15] Mozzone, L., Berni, A. Long range, large throughput radio data link for DUSS (Deployable Underwater Surveillance Systems). SACLANTCEN Memorandum SM-360. La Spezia, Italy, NATO SACLANT Undersea Research Centre, 1999.
- [16] Mozzone, L. Shallow water surveillance with deployable sonar systems. *Naval Forces 6/97*, 1997, Monch Publishing Group.

[17] Mozzone, L., Bongi, S. Localization and fusion of echoes with deployable multistatic active sonar: evaluation of feasibility using experimental data. 4th European Conference on Underwater Acoustics, 1998, Rome, Italy.

[18] Mozzone, L., Bongi, S. Deployable multistatic active sonar: the cycle of system design, tests and data analysis, IEEE Oceans '98 Conference, 1998, Nice, France.

[19] Mozzone, L., Bongi, S. Deployable Underwater Surveillance Systems for ASW: experimental results at NATO SACLANT Centre. Underwater Defense Technology UDT'98 Classified Conference, London, UK.

## Annex A - Equation of models

The equations used in Monte Carlo simulation for time-only, bearing only and AUV localization methods are shown here.

### A.1 Time-only localization method model ("Tri-lateration")

The figure below represents the model used for all time-only localization simulations. The source/receiver n.1 are represented in Fig. A1 with point B and receiver n.2 is represented with point C. Point A is the real position of the target and point A' indicates the position estimated with the equations reported below.

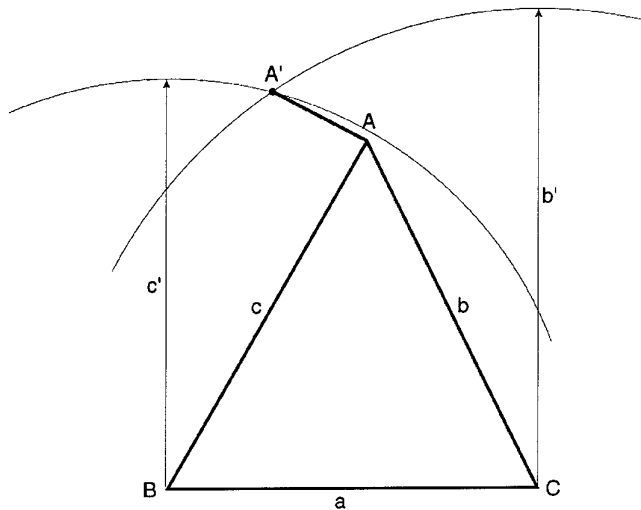


**Figure A1** Geometric scheme of time-only localization model

#### A.1.1 Precision of $\tau_1$ and $\tau_2$

$$\tau_1 = \frac{2 \cdot c}{v_c} \quad (\text{A.1})$$

$$\tau_2 = \frac{c+b}{v_c} \quad (\text{A.2})$$

$\tau_1$  and  $\tau_2$  are the travel time (source-target-receiver) for the real position and  $v_c$  is the sound velocity.  $\tau'_1$  and  $\tau'_2$  are the travel time (source-target-receiver) for the target position disturbed by a Gaussian error N.

$$\tau'_1 = \tau_1 + N(0, \sigma_{\tau_1}) \quad (\text{A.3})$$

$$\tau'_2 = \tau_2 + N(0, \sigma_{\tau_2}) \quad (\text{A.4})$$

$$c' = \frac{\tau'_1 \cdot v_c}{2} \quad (\text{A.5})$$

$$b' = \tau'_2 \cdot v_c - c' \quad (\text{A.6})$$

The intersection between two circles (one of centre in B and radius  $c'$  and the other of centre in C and radius  $b'$ ) determine the estimated position of target in the time-only localization method discussed here. The length of segment AA' is the error between the real position and the estimated position of the target.

#### A.1.2 Precision of $\tau_1$ and $\tau_2$ in AUV model

In this case point B and C represent the receiver 1 and receiver 2 and point A is the target with an active pinger.

$$\tau_1 = \frac{c}{v_c} \quad (\text{A.7})$$

$$\tau_2 = \frac{b}{v_c} \quad (\text{A.8})$$

$\tau_1$  and  $\tau_2$  are travel time (target-receiver) for real position and  $v_c$  is velocity of sound.

$$\tau'_1 = \tau_1 + N(0, \sigma_{\tau_1}) \quad (\text{A.9})$$

$$\tau'_2 = \tau_2 + N(0, \sigma_{\tau_2}) \quad (\text{A.10})$$

$\tau'_1$  and  $\tau'_2$  are travel time (target-receiver) disturbed by a Gaussian error N.

$$c' = \tau'_1 \cdot v_c \quad (\text{A.11})$$

$$b' = \tau'_2 \cdot v_c \quad (\text{A.12})$$

The intersection between two circles (one of centre in B and radius  $c$  and the other of centre in C and radius  $b$ ) determine the estimated position of target in AUV localization method). The length of segment AA' is the error between real position and estimated position of target.

#### A.1.3 Position of buoy

$$B' = B + N(0, \sigma_{POS}) \quad (A.13)$$

$B'$  is the new position of the buoy obtained from the real position adding a Gaussian error. The intersection between two circles (one of centre in  $B'$  and radius  $c$  and the other of centre in C and radius  $b$ ) determine the estimated new position of the target ( $A'$ ). The distance between real position (A) and calculated position ( $A'$ ) determine the error produced by the error on buoy position introduced above.

#### A.1.4 Estimation of $v_c$ (velocity of sound)

$$v_c' = v_c + N(0, \sigma_{v_c}) \quad (A.14)$$

$v_c'$  is new velocity of sound obtained adding a noise to the real velocity  $v_c$

$$c' = \frac{\tau_1 \cdot v_c'}{2} = \frac{2 \cdot c \cdot v_c'}{2 \cdot v_c} = \frac{c}{v_c} \cdot v_c' \quad (A.15)$$

$$b' = \tau_2 \cdot v_c' - c = \frac{c+b}{v_c} \cdot v_c' - \frac{c}{v_c} \cdot v_c' = \frac{b}{v_c} \cdot v_c' \quad (A.16)$$

The intersection between two circles (one of centre in B and radius  $c'$  and the other of centre in C and radius  $b'$ ) determine the estimated new position of target ( $A'$ ). The distance between real position (A) and calculated position ( $A'$ ) determine the error produced by the error on  $v_c$  introduced above.

## A.2 Bearings only localization model ("Tri-angulation")

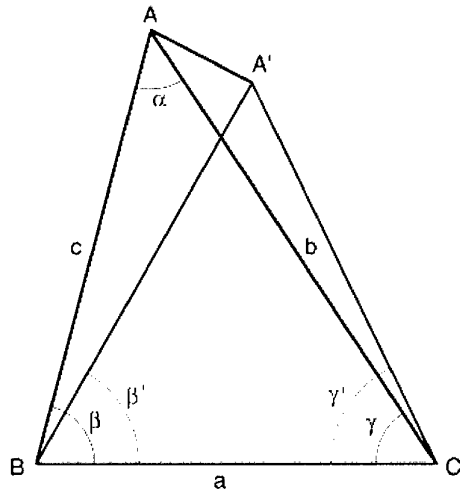


Figure A2 Geometric scheme of bearing-only localization model

From the cosine theorem:

$$\cos \alpha = \frac{b^2 + c^2 - a^2}{2 \cdot b \cdot c} \Rightarrow \alpha = \cos^{-1} \frac{b^2 + c^2 - a^2}{2 \cdot b \cdot c} \quad (\text{A.17})$$

From the sine theorem:

$$\sin \gamma = \frac{c}{a} \cdot \sin \alpha \Rightarrow \gamma = \sin^{-1} \frac{c}{a} \cdot \sin \alpha \quad (\text{A.18})$$

Form identity triangle relation: (A.19)

$$\beta = \pi - (\alpha + \gamma) \quad (\text{A.20})$$

$$\beta' = \beta + N(0, \sigma_{\theta_1}) \quad (\text{A.21})$$

$$\gamma' = \gamma + N(0, \sigma_{\theta_2}) \quad (\text{A.22})$$

$\beta'$  and  $\gamma'$  are the new angles obtained adding two normal distribution at real angle

$$y - y_B = m_1 \cdot (x - x_B) \text{ with } m_1 = \tan \beta' \quad (\text{A.23})$$

$$y - y_c = m_2 \cdot (x - x_c) \text{ with } m_2 = \tan \gamma' \quad (\text{A.24})$$

The intersection between two lines of equation A.23 and A.24 is the estimated position of target in tri-angulation method. The length of segment  $AA'$  is the error between real position and estimated position of the target.

### A.3 Three buoys model

In this case there are three buoys: one source/receiver and two receivers in a triangle. The buoys are represented in Fig. A3 with point B for source/receiver and point C and D for the other receivers.

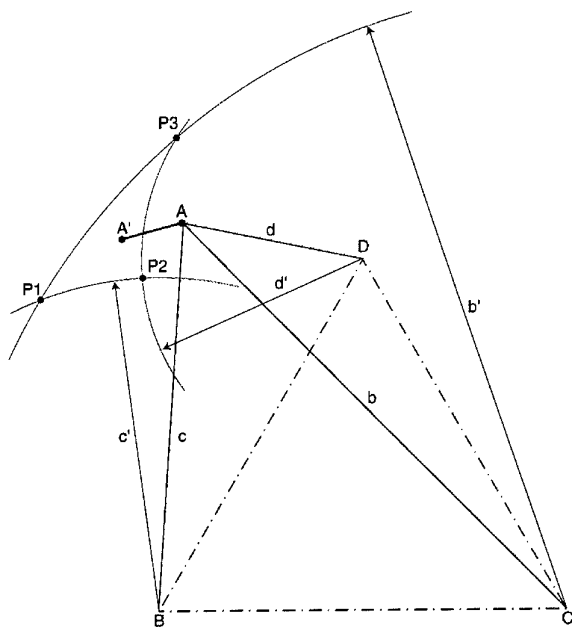


Figure A3 Geometric scheme of tri-lateration model with three buoys.

#### A.3.1 Time-only localization

$$\tau_1 = \frac{2 \cdot c}{v_c} \quad (\text{A.25})$$

$$\tau_2 = \frac{c + b}{v_c} \quad (\text{A.26})$$

$$\tau_3 = \frac{c+d}{v_c} \quad (\text{A.27})$$

$\tau_1, \tau_2$  and  $\tau_3$  are the travel time (source-target-receiver) for the real target position A and  $v_c$  is the sound velocity.

$$\tau_1' = \tau_1 + N(0, \sigma_{\tau_1}) \quad (\text{A.28})$$

$$\tau_2' = \tau_2 + N(0, \sigma_{\tau_2}) \quad (\text{A.29})$$

$$\tau_3' = \tau_3 + N(0, \sigma_{\tau_3}) \quad (\text{A.30})$$

$\tau_1', \tau_2'$  and  $\tau_3'$  are the travel time (source-target-receiver) for a target positions disturbed by a Gaussian error:

$$c' = \frac{\tau_1' \cdot v_c}{2} \quad (\text{A.31})$$

$$b' = \tau_2' \cdot v_c - c' \quad (\text{A.32})$$

$$d' = \tau_3' \cdot v_c - c' \quad (\text{A.32})$$

Solutions are obtained as the intersections of three pairs of circles (one of centre in B and radius  $c'$  plus one of centre in C and radius  $b'$  determine P1), (one of centre in B and radius  $c'$  plus one of centre in D and radius  $d'$  determine P2), (one of centre in C and radius  $b'$  plus one of centre in D and radius  $d'$  determine P3). The geometric centre of the three points represents the estimated position of the target in the time-only localization method with three buoys. The length of segment AA' is the error between real position and estimated position of target.

### A.3.1 AUV localization

In this case point B, C and D represent the receiver n.1, receiver n.2 and receiver n.3 and point A is the target with an active pinger.

$$\tau_1 = \frac{c}{v_c} \quad (\text{A.33})$$

$$\tau_2 = \frac{b}{v_c} \quad (\text{A.34})$$

$$\tau_3 = \frac{d}{v_c} \quad (\text{A.35})$$

$\tau_1, \tau_2$  and  $\tau_3$  are travel times (target-receiver) for real position A and  $v_c$  is velocity of sound.

$$\tau_1' = \tau_1 + N(0, \sigma_{\tau_1}) \quad (\text{A.36})$$

$$\tau_2' = \tau_2 + N(0, \sigma_{\tau_2}) \quad (\text{A.37})$$

$$\tau_3' = \tau_3 + N(0, \sigma_{\tau_3}) \quad (\text{A.38})$$

$\tau_1', \tau_2'$  and  $\tau_3'$  are travel time (target-receiver) for wrong positions of target

$$c' = \tau_1' \cdot v_c \quad (\text{A.39})$$

$$b' = \tau_2' \cdot v_c \quad (\text{A.40})$$

$$d' = \tau_3' \cdot v_c \quad (\text{A.41})$$

Solutions are obtained as the intersections of three pairs of circles (one of centre in B and radius  $c'$  plus one of centre in C and radius  $b'$  determine P1), (one of centre in B and radius  $c'$  plus one of centre in D and radius  $d'$  determine P2), (one of centre in C and radius  $b'$  plus one of centre in D and radius  $d'$  determine P3). The geometric centre of the three points represents the estimated position of the target in the AUV localization method with three buoys. The length of segment AA' is the error between real position and estimated position of target.

## Annex B - Contact localization data

This annex shows all the plots described in Sect. 3.1. Note: \*some plots are out of scale .

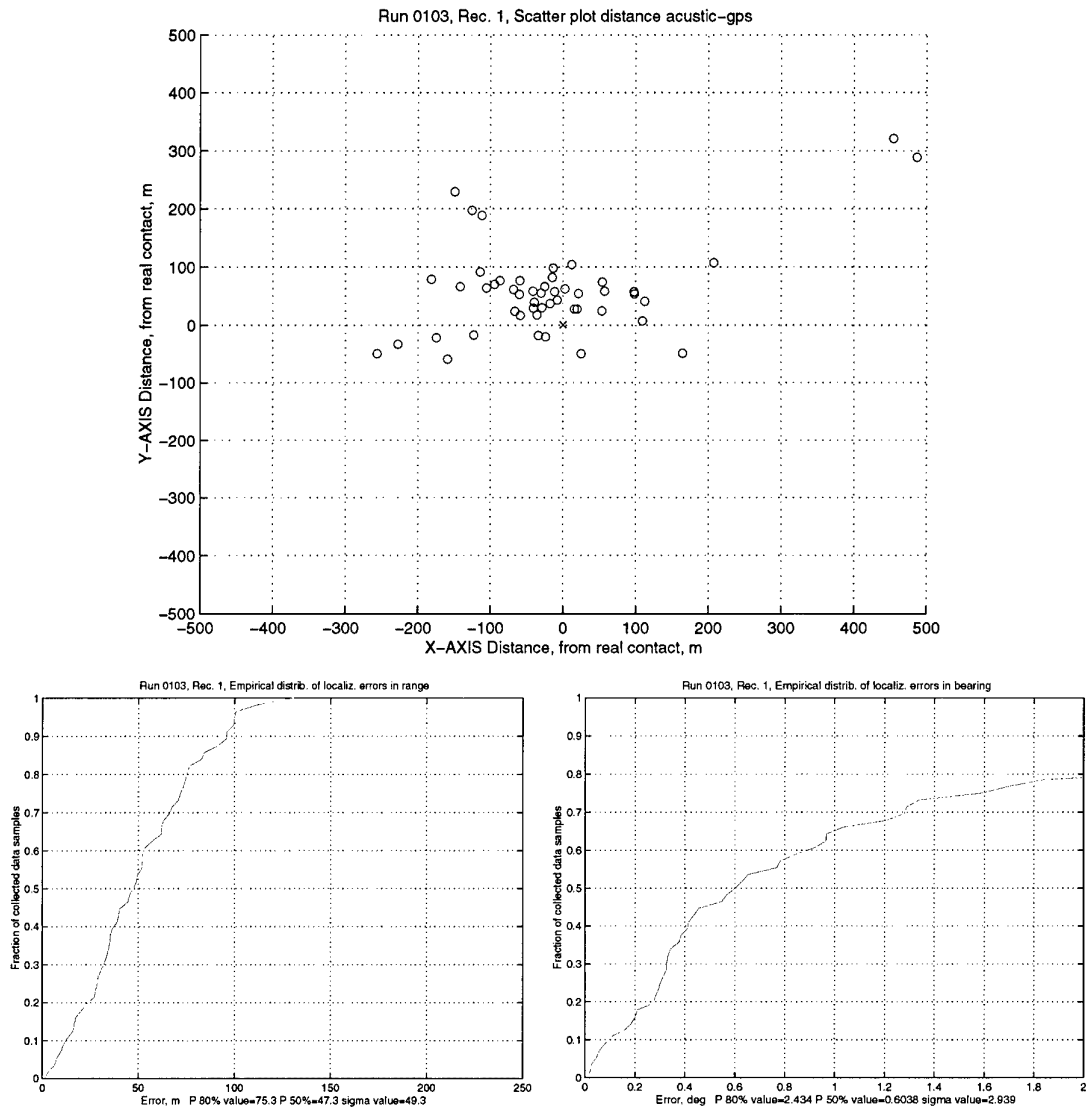


**Figure B1** RUN 0103, Receiver 1: scatter-plot of estimated echo location and empirical distribution of range and bearing errors.

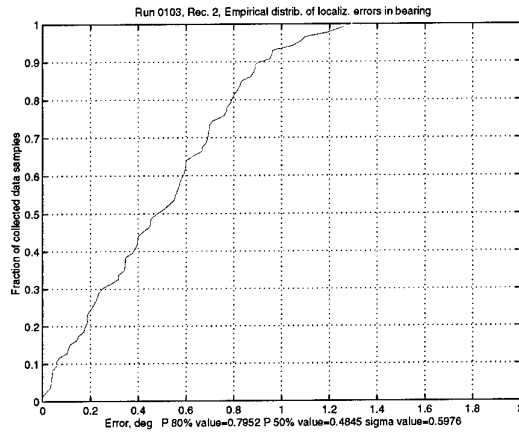
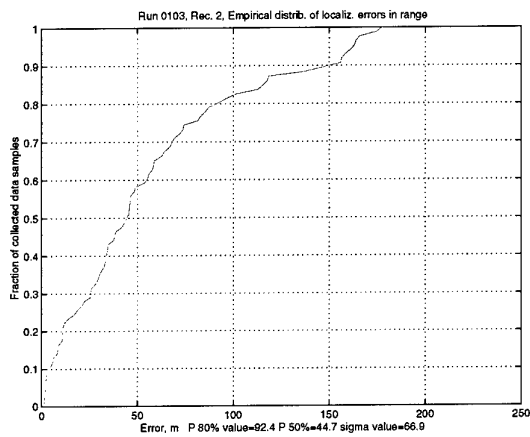
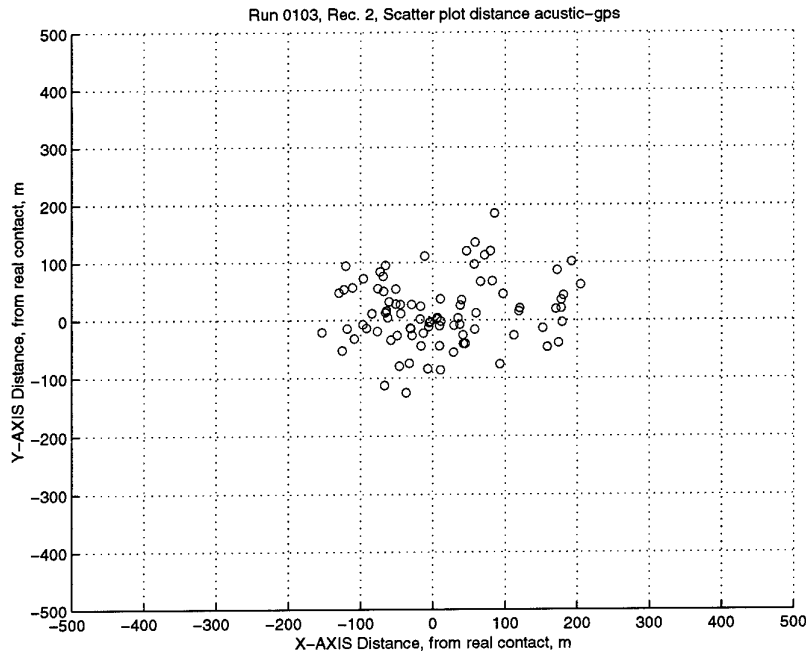


**Figure B2** RUN 0103, Receiver 2: scatter-plot of estimated echo location and empirical distribution of range and bearing errors.

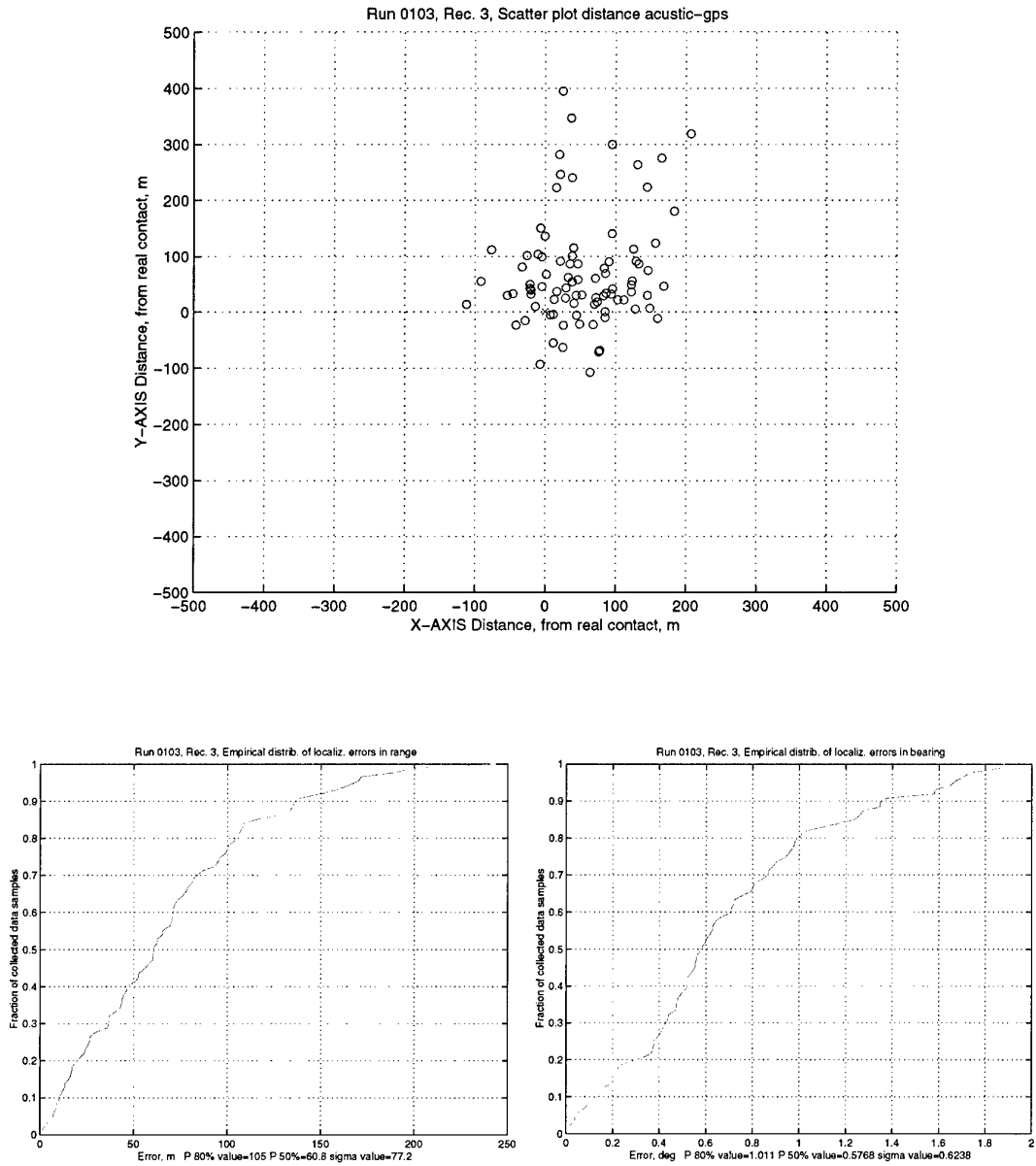


**Figure B3** RUN 0103, Receiver 3: scatter-plot of estimated echo location and empirical distribution of range and bearing errors.

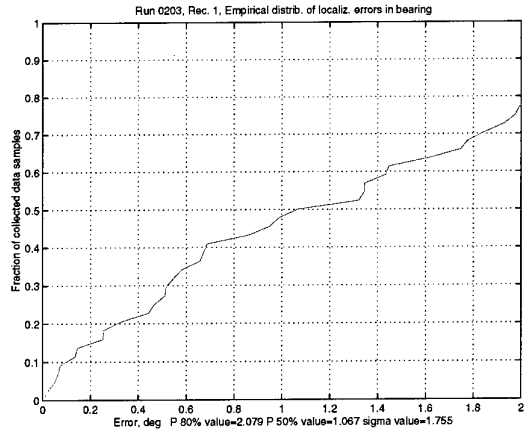
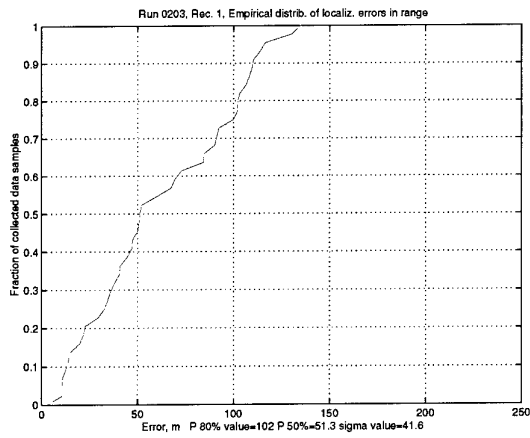
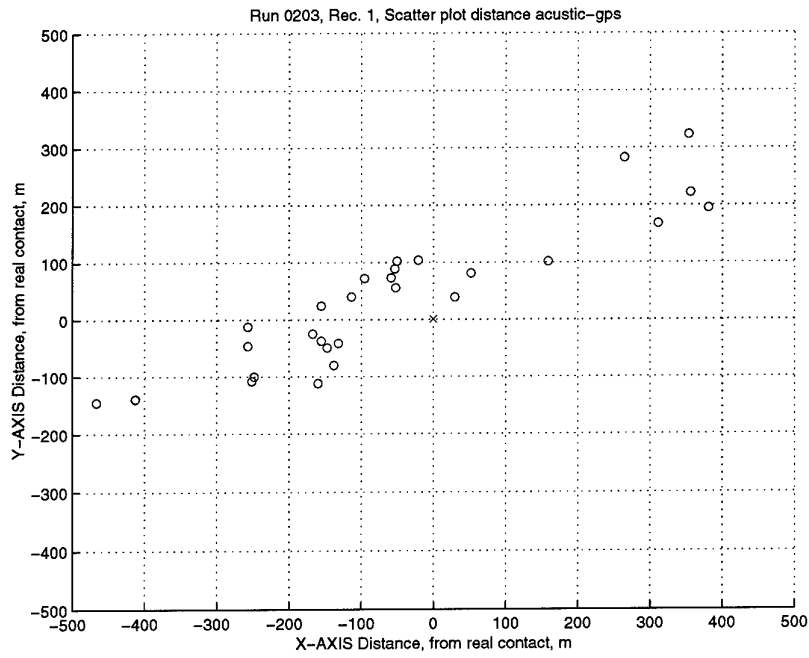


**Figure B4** RUN 0203, Receiver 1: scatter-plot of estimated echo location and empirical distribution of range and bearing errors.

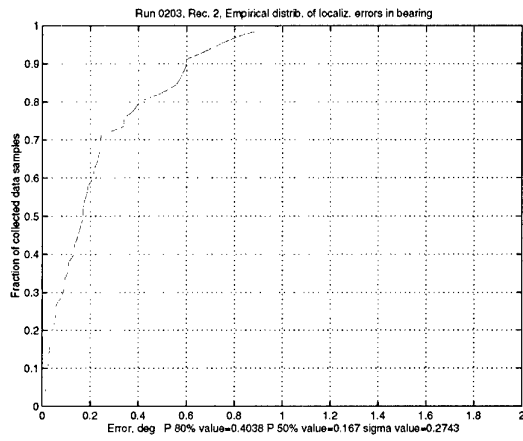
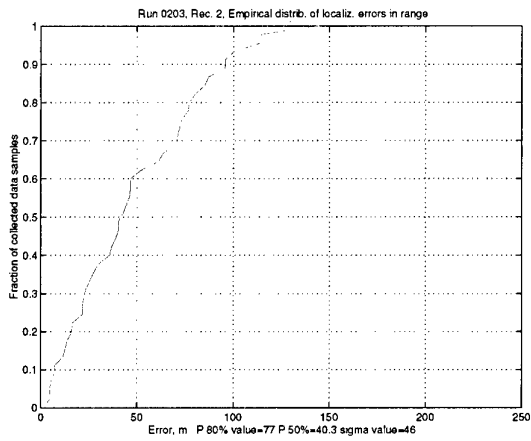
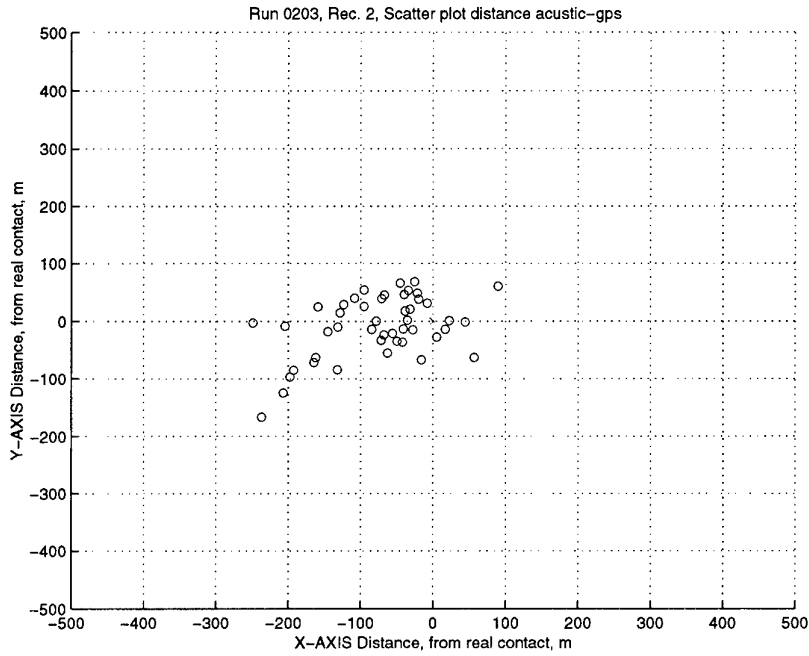


**Figure B5** RUN 0203, Receiver 2: scatter-plot of estimated echo location and empirical distribution of range and bearing errors.

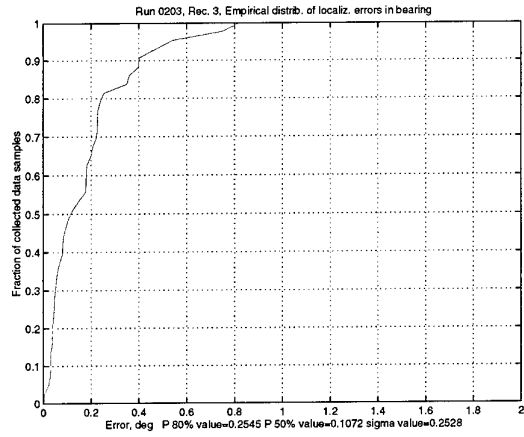
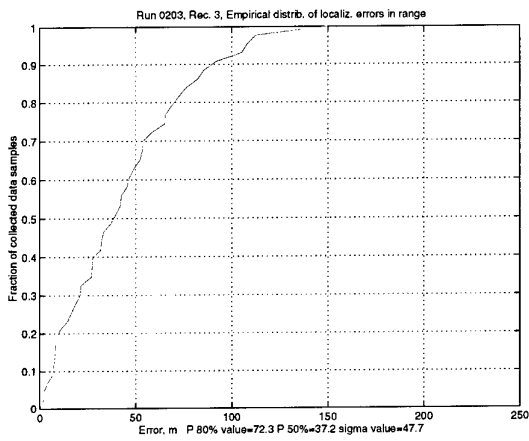
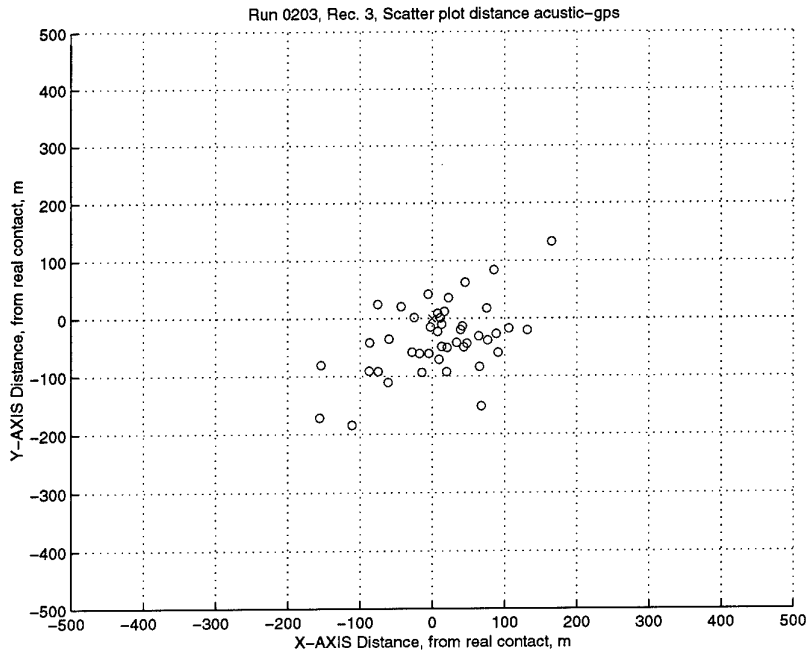


**Figure B6** RUN 0203, Receiver 3: scatter-plot of estimated echo location and empirical distribution of range and bearing errors.

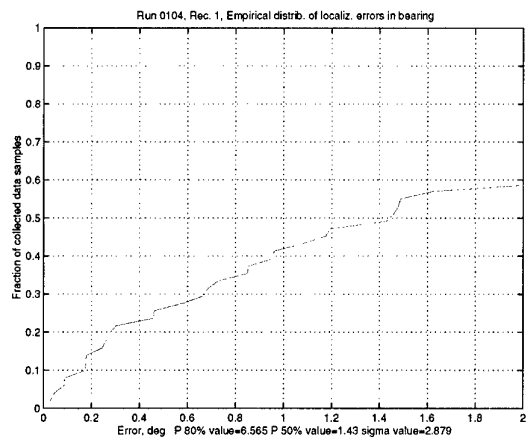
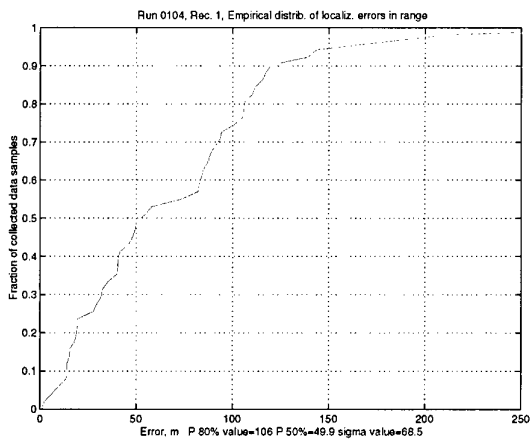
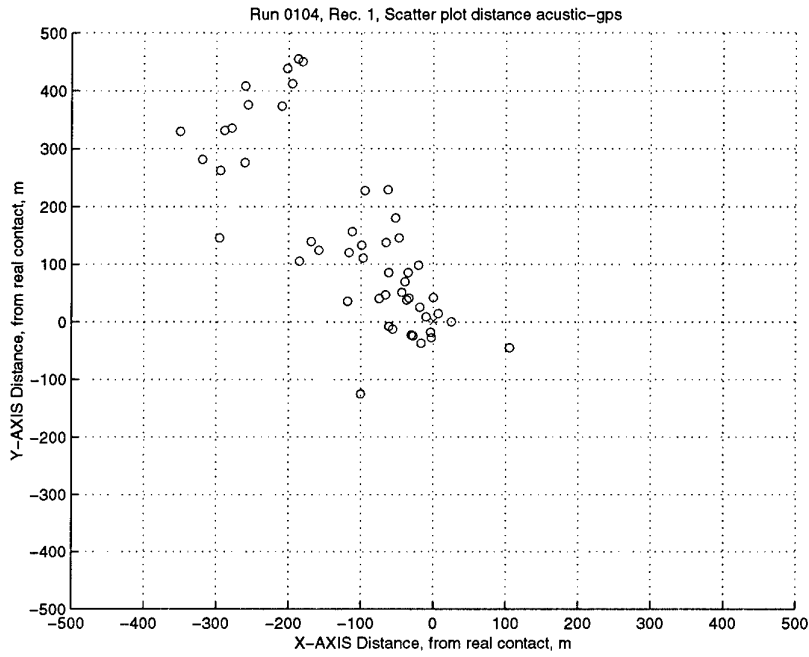


**Figure B7** RUN 0104, Receiver 1: scatter-plot of estimated echo location and empirical distribution of range and bearing errors.

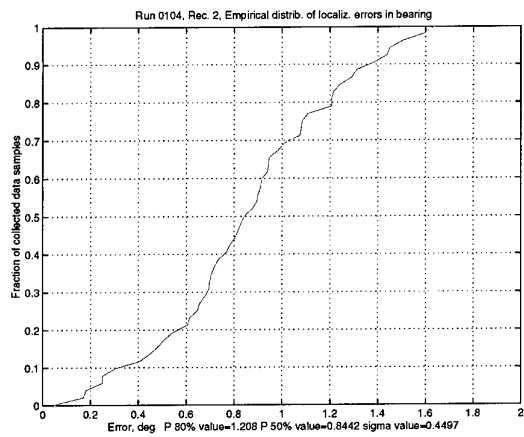
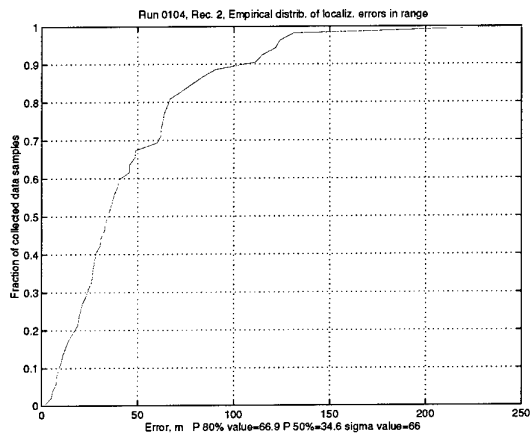
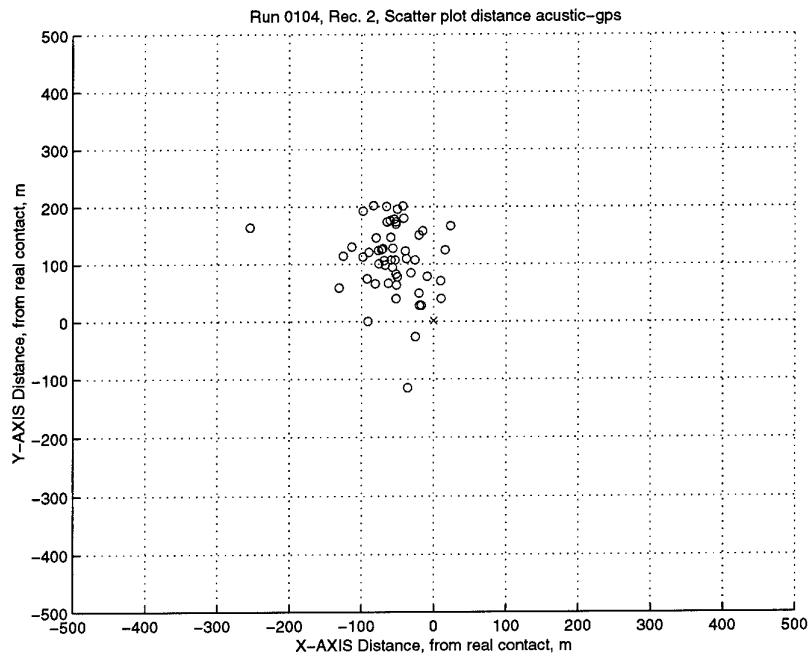


**Figure B8** RUN 0104, Receiver 2: scatter-plot of estimated echo location and empirical distribution of range and bearing errors.

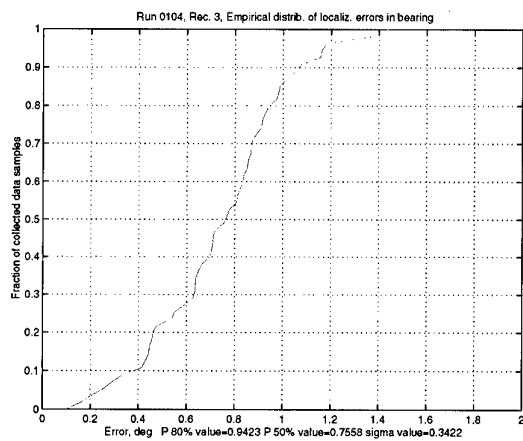
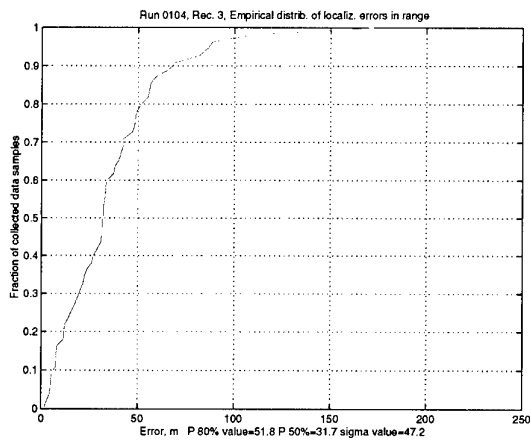
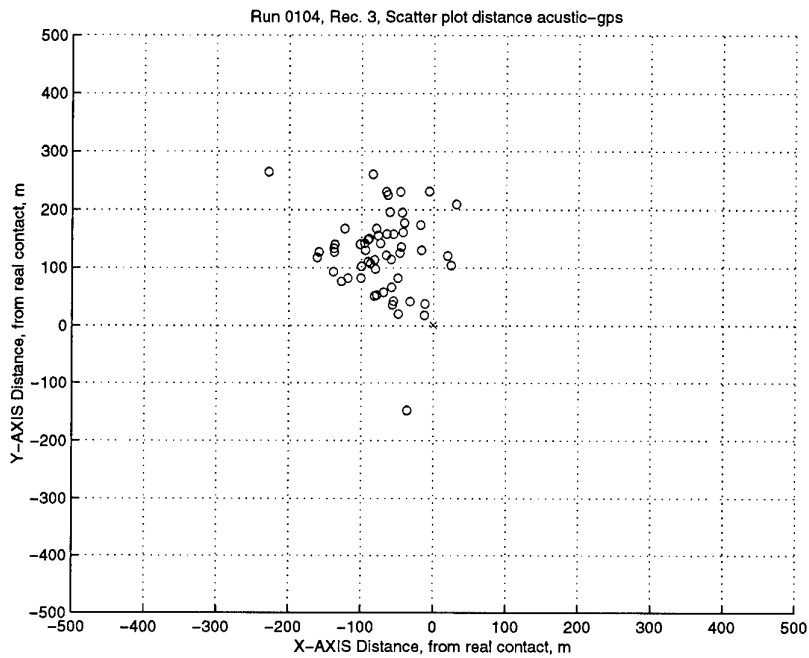


**Figure B9** RUN 0104, Receiver 3: scatter-plot of estimated echo location and empirical distribution of range and bearing errors.

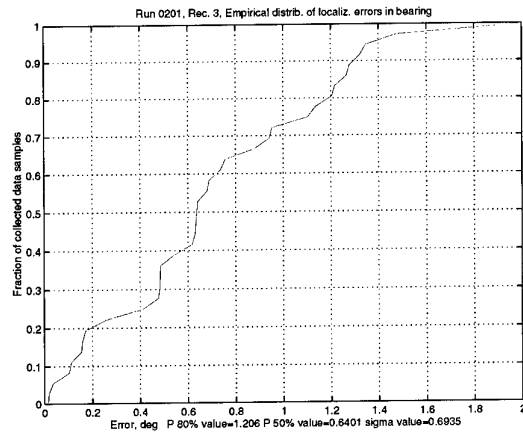
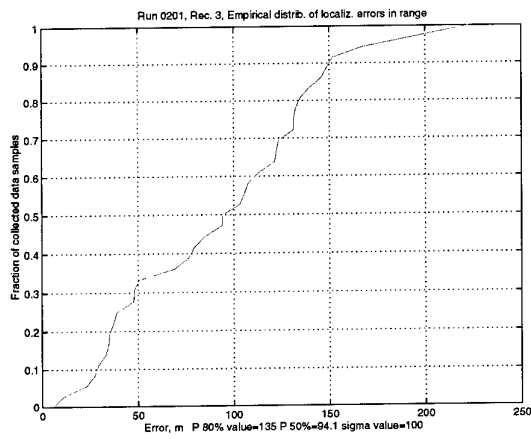
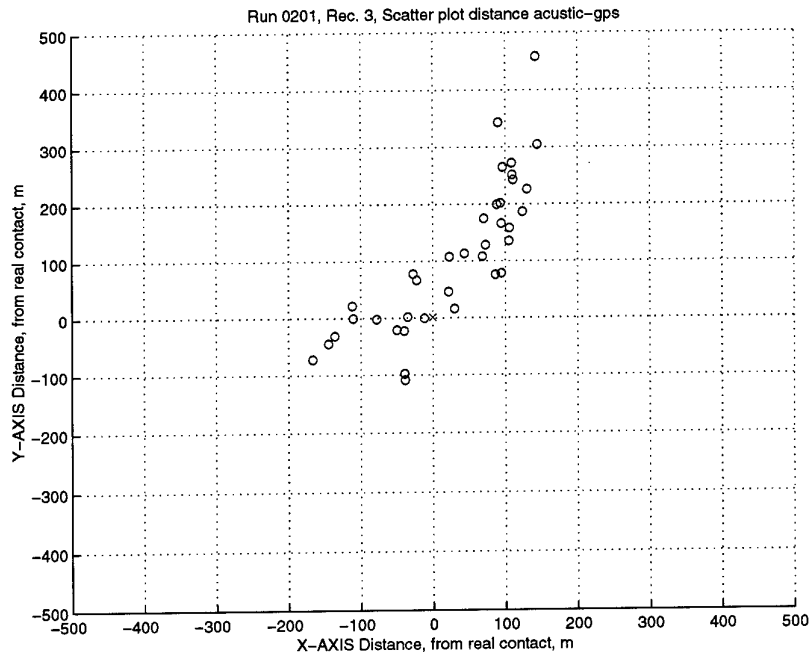


**Figure B10** RUNS 0201, Receiver 3: scatter-plot of estimated echo location and empirical distribution of range and bearing errors.

## Document Data Sheet

<i>Security Classification</i> UNCLASSIFIED		<i>Project No.</i> 04-B
<i>Document Serial No.</i> SR-317	<i>Date of Issue</i> October 1999	<i>Total Pages</i> 60 pp.
<i>Author(s)</i> Mozzone, L., Lorenzelli, P.		
<i>Title</i> Target localization with multiple sonar receivers.		
<i>Abstract</i> <p>Deployable Underwater Surveillance Systems (DUSS) are a network of small multistatic transmitter / receiver sonar nodes. This study analyzes the contact localization capabilities of DUSS in term of range, time and bearing error. This information is used in Monte Carlo simulations to estimate the accuracy of multistatic localization methods using 2 or 3 receivers. Simulations are validated by real data. Time – only localization of active sonar echoes with 2 receivers produces error estimates of 150 m at 10 km. Active pinger localization with 2 receivers produces average errors of 83 m at 10 km. Bearings – only passive localization with 2 receivers produces average errors of 250 m at 10 km. Buoy separation, buoy localization accuracy, acoustic travel time estimation, beam width and compass accuracy are the most critical system parameters. The use of three receivers further improves accuracy.</p>		
<i>Keywords</i> Range – time – bearing – localization – multistatic – sonar – modelling – experiment - AUV		
<i>Issuing Organization</i> North Atlantic Treaty Organization SACLANT Undersea Research Centre Viale San Bartolomeo 400, 19138 La Spezia, Italy  [From N. America: SACLANTCEN (New York) APO AE 09613]		Tel: +39 0187 527 361 Fax: +39 0187 527 700  E-mail: library@saclantc.nato.int

The SACLANT Undersea Research Centre provides the Supreme Allied Commander Atlantic (SACLANT) with scientific and technical assistance under the terms of its NATO charter, which entered into force on 1 February 1963. Without prejudice to this main task - and under the policy direction of SACLANT - the Centre also renders scientific and technical assistance to the individual NATO nations.

---

This document is approved for public release.  
Distribution is unlimited

---

SACLANT Undersea Research Centre  
Viale San Bartolomeo 400  
19138 San Bartolomeo (SP), Italy

tel: +39 0187 527 (1) or extension  
fax: +39 0187 527 700

e-mail: [library@saclantc.nato.int](mailto:library@saclantc.nato.int)

NORTH ATLANTIC TREATY ORGANIZATION